1-1-2008

Wavelet application in acoustic emission signal detection of wire related events in pipeline

Ran Wu
Ryerson University

WAVELET APPLICATION IN ACOUSTIC EMISSION SIGNAL DETECTION OF WIRE RELATED EVENTS IN PIPELINE

by

Ran Wu
Bachelor of Engineering Degree in Electrical and Information Engineering, Beihang University, China, 2004

A thesis
presented to Ryerson University
in partial fulfillment of the
requirement for the degree of
Master of Applied Science
in
Electrical and Computer Engineering.

Toronto, Ontario, Canada, 2008

Author's Declaration

I hereby declare that I am the sole author of this thesis.
I authorize Ryerson University to lend this thesis to other institutions or individuals for the purpose of scholarly research.

Signature

I further authorize Ryerson University to reproduce this thesis by photocopying or by other means, in total or in part, at the request of other institutions or individuals for the purpose of scholarly research.

Signature

Ryerson University requires the signatures of all persons using or photocopying this thesis. Please sign below, and give address and date.

Wavelet Application in Acoustic Emission Signal Detection of Wire Related Events in Pipeline, 2008, Ran Wu, Electrical and Computer Engineering, Ryerson University.

Abstract

This thesis establishes an automatic classification program for the signal detection work in pipeline inspection. Time-scale analysis provides the basic methodology of this thesis work. The wavelet transform is implemented in the program for filtering out the majority of noise and detect needed signals.

As a popular nondestructive test, acoustic emission (AE) testing has been widely used in many physical and engineering fields such as leak detection and pipeline inspection. Among those applied AE tests, a common problem is to extract the physical features of the ideal events, so as to detect similar signals. In acoustic signal processing, those features can be represented as joint time-frequency distribution. However, classical signal processing methods only give global information on either time or frequency domain, while local information is lost. Although the short-time Fourier transform (STFT) is developed to analyze time and frequency details simultaneously, it can only achieve limited precision. Other time-frequency methods are also applied in AE signal processing, but they all have the problem of resolution and time consuming.

Wavelet transform is a time-scale technique with adaptable precision, which makes better feature extraction and detail detection. This thesis is an application of wavelet transform in AE signal detection where various noise exists. The wavelet transform with Morelet wavelet as the mother wavelet provides the basis of the program for auto classification in this thesis work. Finally the program is tested with two industrial projects to verify the workability of wavelet transforms and the reliability of the developed auto classifiers.

Acknowledgments

Many thanks to my supervisors, Dr. Lian Zhao and Dr. Zaiyi Liao, for their professional directions, essential comments and kind supports.

This work is partially supported by Ontario Center of Excellence (OCE), Pressure Pipe Inspection Company Ltd. (PPIC) under grant number RY-EE-M50196-07, and Ryerson University. Special thanks to Theresa R. Erskine at the Research Office of Ryerson University, who bridges our collaboration with PPIC.

Also thanks a lot to Cameron White and Xiangjie Kong in PPIC for the data and their help.

Finally, I'm grateful to my labmate Lu Bai for her constructive advices and nice supports.

Contents

List of Tables

List of Figures

Chapter 1

Introduction

This thesis is based on the work of signal analysis and detection for the patent Acoustic Emission Testing (AET) data provided by our industry partner, Pressure Pipe Inspection Company Ltd. (PPIC).

The company uses acoustic emission (AE) testing which is a non-destructive testing method to monitor the condition of pipeline. All the acoustic signals recorded by sensors in AE monitoring need to be further processed to extract needed ones. However, usually the percentage of real needed signals are less than 1%. This means, the company has to hire many analysts to filter ideal signals out of plenty of noise signals. Moreover, the method that the company currently using is a short-time Fourier transform(STFT) software. After processed with the software, the output of the analyzed signal is a two dimension time-frequency plotting. Analysts have to differentiate and filter signals via observing the plotting as well as listening to the original acoustic signals. Generally speaking, it costs analysts a lot of time to do the filtering work manually. 2 minutes per signal is required as average. In each day of the monitoring over 500 signals are coming in. Thus, several hours are spent on the analyzing work every day, excluding the accuracy issue resulted from the fatigue and boredom of this repeating work.

The algorithm presented in this thesis basically focuses on classifying the recorded signals into defined groups automatically and accurately. In addition, a friendly user interface is designed in the implementation to allow analysts immediately use the software. Furthermore,

the efficiency of the algorithm provides the basis and possibility of hardware implementation for embedded systems.

This chapter is organized as the following:

- Section 1.1 provides an snapshot of the whole chapter, including AE basis and an introduction to time-frequency analysis and wavelet transform.
- Section 1.2 and 1.3 give a brief background of general AE testing procedure and characteristics.
- Section 1.4 introduces the time-frequency representation and analysis for AE signal processing.
- Section 1.5 explains the time-scale analysis and introduces the wavelet transform which is implemented for the whole thesis work.
- Section 1.6 describes the proposed work and motivation.
- The contribution and outline of the thesis is covered in the last section.

1.1 Overview

AE testing has been widely used in physical and architecture fields due to its efficiency, reliability and low operation costs. In steel pipelines, when a present defect expands, tension energy is released, and an acoustic signal is generated [1]. AE techniques are used to observe and monitor these invisible events. Although some of the events occur before monitoring, or are too weak to be detected during inspection, various events occur due to temperature, pressure, physical defect development and environmental conditions so that they become detectable. Previous studies showed that the amplitude of AE signal is proportional to the released energy [2], and the frequency distribution is related with the size of the defect [3]. For instance, in leak detection of a pipeline, the AE signal detected from larger leak hole contains more low frequency components. An explanation of this phenomenon is that larger hole creates smaller pressure, which results in lower frequency components.

The AE events that occur in pipeline usually create two types of signals: one is a mechanical wave which propagates along the steel wire in the pipe at high frequency (above 100 kHz), another is a low frequency wave (about 30 kHz) that propagates through the medium (gas or liquid) inside the pipe. Stulen and Muravev show in their research [1, 4] that the attenuation of the waves has a square relationship with their frequency, and the coefficient of this relationship is distinguished by the particular medium. Observed values for attenuation (in dB/ft) in several gases and water are $4.9 \times 10^{-11} f^2$ and $7.8 \times 10^{-14} f^2$, respectively, where f is the frequency. Therefore, AE signals propagating through the steel wire attenuate very quickly because the frequency is high. However, those low frequency waves that propagate in the medium can be detected even at sites hundreds of meters away from the original signals. In addition, this kind of wave interacts with the pipe wall so that it can be detected by sensors mounted outside of the pipe.

For AE signal detection and feature extraction, many acoustic signal processing methods have been used. Classical frequency analysis [3] gives global information about the signal, such as spectrum, frequency peaks and signal-to-noise ratio(SNR), which makes the detection work ambiguous. In fact, time variant features that can be depicted by changing signal frequency components with time, is the main characteristic of acoustic signals. This is similar to music composition. Each musical tone is the combination of certain frequency bands, and different tones arrive at different time to make the music. Hence, we need to know the arrival time and location of those frequency components in the time domain, in order to discriminate different AE signals and detect the right events. Therefore, in the time-frequency plane, these local details are much more important than global information.

This requirement cannot be satisfied by classical Fourier transform. To solve this time-frequency problem, Short-time Fourier transform (STFT) was applied to signal processing [5]. STFT uses small windows to localize a signal in the time domain, and then applies Fourier transform to get the frequency distribution only in this window. However, this STFT window, or atom, has certain size and precision restrictions, which locks the time-frequency analysis at a certain resolution level. The wavelet transform, which was first created in

seismology, was introduced to signal processing to solve this multi-resolution problem [6].

As a well known methodology that has been developed for over ten years, Wavelet Transform (WT) is an advanced technique in signal processing field. Its prominent capability in feature extraction and detail detection has been proven and used in various application fields. In traditional signal processing fields such as speech signal processing [7] and image processing [8], WT played an important role in denoising, signal recognizing and classification, as well as feature extraction. In addition, WT is applied in plenty of modern cross fields including bioengineering [9], medicine [10] and mechanical fields [11].

1.2 Acoustic Emission Testing

1.2.1 Introduction to Acoustic Emission

AE technique is one of the most unique approaches among all the non-destructive testing (NDT) methods. NDT are noninvasive techniques aiming to determine the integrity, component or structure of a material or quantitatively measure some characteristic of an object. In contrast to destructive testing, NDT does no harm to the test object [12]. Among all the NDT methods such as magnetic testing, penetrant testing, ultrasonic testing and radiographic testing, AE plays a distinctive role which is usually applied during loading of a structure, while most of the others are applied before or after loading. AE is a dynamic technique that works when solid materials lose their elasticity and just begin to split, while other NDT methods are static. For example the ultrasound method, which is a typical NDT technique, is able to detect the geometric shape of a defect in a specimen using an artificially generated source signal and a receiver, whereas the AET detects the elastic waves radiated by a growing fracture [13].

When other NDT techniques probe the structure, AE listens for emissions from active defects and splits. It is the class of phenomena whereby an elastic wave is generated by the rapid release of energy from the source in a material. The elastic wave, normally between 10 KHz and 1MHz, propagates through the solid material to the surface where it can be detected by one or more sensors [14]. The sensor is a transducer which converts the mechanical wave

into an electrical signal. Then this signal can be processed and localized to extract the source of the AE events. Consequently, AE is a very sensitive NDT technique to observe damage processes during the entire observation without any disturbance to the specimen.

AE can be deployed in a wide range of usable applications of NDT such as [15]:

- AE on metal pressure vessels for cracks and corrosion;
- AE on piping systems for splits and leakage;
- AE on flat bottomed storage tanks for leakage and corrosion;
- AE on civil-engineering structures for process monitoring and global or local long-term monitoring.

It should be noted that the test conditions for all the applications must be similar to normal service conditions. Otherwise AE will not obtain veritable and reliable results.

1.2.2 Main Characteristics of AE

Source of AE:

NDT methods are used to explore the structure of solid materials. AE is especially used to monitor the occurrence of defects.

All solid materials, both rigid and elastic, have certain elasticity. They become strained under external forces, and spring back when released [16]. Higher force makes heavier deformation, thus, the elastic energy is greater. Also corrosion decreases the sustainable limit of the material. When the energy is large enough and the elastic limit is exceeded, a fracture happens immediately if it is a brittle material, or occurs after a certain plastic deformation if it is a longsuffering material. The occurred fracture rapidly relaxes the material by a fast dislocation. This kind of rapid release of elastic energy is defined as an AE event. It generates an elastic wave that propagates and can be detected by sensors. The frequency of this wave has a very wide range depending on the material. For example the frequency of AE testing of metallic objects is in the range of ultrasound above 100 kHz.

The sound of glasses crack is familiar to us as the frequency is inside sound wave range. When the tiny crack occurred to metal or some other solid materials, it is not hearable as the emitted burst is ultrasound. This type of pulses and bursts are one of the sources that AE testing is hunting for. Another type comes from the plastic deformation. During the deformation, dislocations move through the crystal lattice. AE signals are generated from these movements, but most of them only have very small amplitudes. Thus they can be detected reliably only at a short distance and with less noise background. Fortunately, this type of movements produces continuous signals rather than short bursts. The splitting of material contains both these two types. It makes pulses when defect is produced. It also generates continuous waves when the defect is extending. In a word, AE testing is a receptive technique analyzing the pluses and waves emitted by a defect right in the moment of its occurrence [16].

Signal Propagation:

The wave propagates as concentric circles around its source on flat surfaces and can be detected by one or more sensors closest to it. During propagation, the wave is attenuated. As discussed in section 1.1, the attenuation has certain relationship with frequency. Generally speaking, higher frequency waves attenuate faster than low frequency waves. This attenuation also depends on different material and even medium inside the material. Sometimes frequency components are absorbed by distinguished materials.

In linear location case such as pipeline, the wave propagation is more complex due to wave reflection and absorption by the inner wall of the material. In addition, the medium inside the vessel is an essential effect to the propagation of the elastic waves. For example, in pipeline inspection, generated waves propagate through both the solid wall and the medium as mentioned in section 1.1. The propagation through the wall has greater attenuation such that it can not be detected at a distance farther than several meters. While the waves propagated through the medium are much more reliable to be recorded hundreds of meters away. In addition, this propagation is varied in different conditions such as the medium, the

speed of the medium, the temperature, the landscape, etc.

Signal Parameters:

This part provides the original method to characterize AE signals that have been recorded by the sensors. It uses statistical parameters in time domain to help feature extraction and signal classification. Although several more advanced techniques have been applied to this field such as time-frequency analysis and time-scale analysis, this statistic information should be introduced to provide an outlook of the AE signal.

Fig. 1.1 shows the statistic parameters well used in AE testing field:

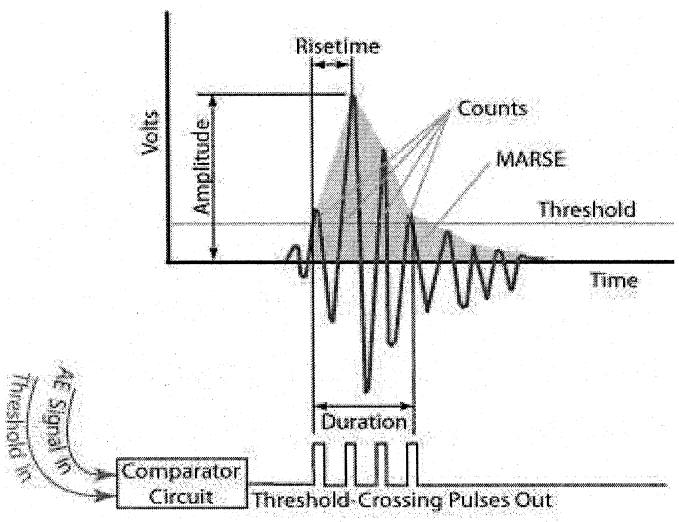

Figure 1.1: Parameters of an AE signal.

1. Amplitude is the highest peak voltage attained by an AE waveform.
2. Counts are the threshold-crossing pulses that counted.
3. MARSE (measured area under the rectified signal envelope) is the measured area under the rectified signal envelope.
4. Duration is the elapsed time from the first threshold crossing to the last.
5. Rise time is the elapsed time from the first threshold crossing to the signal peak.

Source Location:

Usually there are two directions of the source localization of a signal recorded by the two sensors: 1) from the difference of the arrival time; 2) from the difference of the amplitude. The second direction is hard to apply because it is affected by many aspects, which makes the attenuation function for different cases hard to define [4].

Source location techniques assume that AE waves travel at a constant velocity in the same material. The localization of zonal area is more complex than linear area such as pipeline. In the pipeline inspection, once the AE event is recorded by two or more sensors, the difference of arrival time and sound velocity in the material can be used to determine the location of the source.

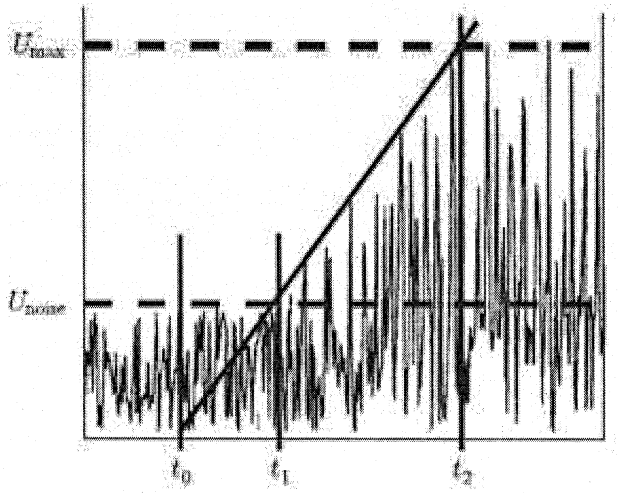

Figure 1.2: Amplitude floating method.

Generally speaking, the arrival time is defined as the start of the duration. It is the first threshold crossing. However, the signal actually starts before the defined arrival time, and this real beginning is concealed by the background noise. Therefore, the uncertainty of arrival time causes certain error of the localization work. To make up this deficiency, many methods are declared. In [4], several methods of determining the genuine arrival time are introduced and compared. Three of them are mostly used: amplitude floating, mutual correlation and two integrals.

- Amplitude Floating:

This method uses threshold to differentiate signal and noise as Fig. 1.2 shows. Then rising function is assumed to be linear so as to calculate the error, and obtain the real arrival of the signal. The disadvantages of the methods are: 1) threshold is hard to artificially define; 2) the edge function is not linear. Usually it is similar to power function, which makes the error increases.

- Mutual Correlation:

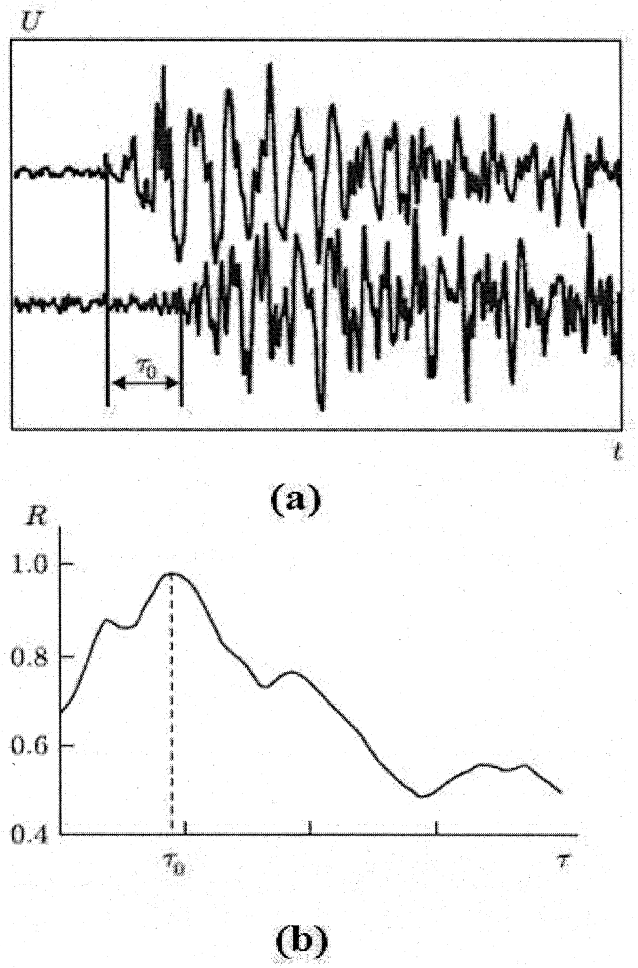

Figure 1.3: Mutual correlation method.

As shown in Fig. 1.3, this method basically calculates the correlation of the two recorded signals from two sensors, and the most possible time difference lays on the largest correlation value.

- Two Integrals:

This method calculates the most rapidly changing part of the signal in time domain, which is most possible to be the arrival of the signal. The illustration is given in Fig. 1.4.

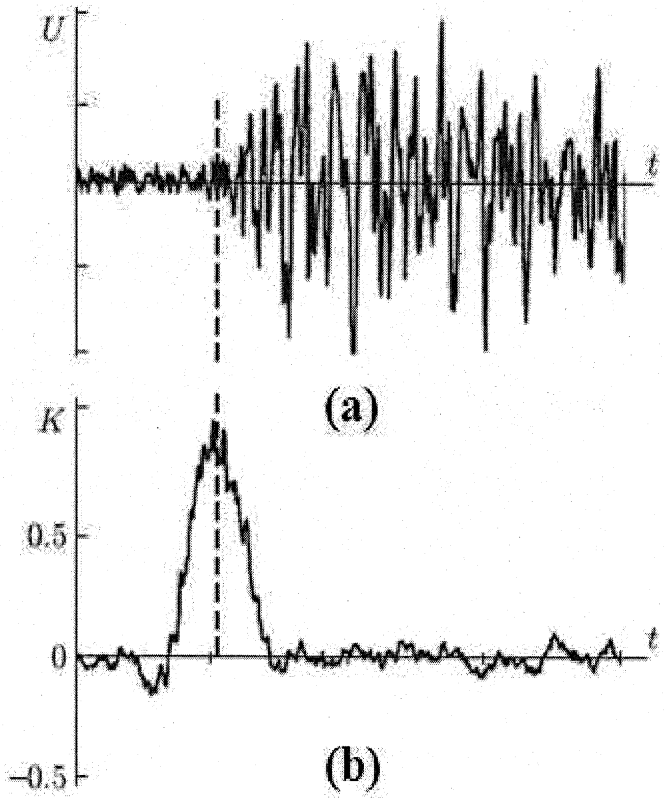

Figure 1.4: Two integrals method.

All of the methods largely depend on the signal-to-noise ratio(SNR) of the signal. If the noise is too large that makes signal hard to be extracted, then the error will greatly increase.

Muravev concludes in [4] as:

Among these three methods, the last one has the highest accuracy. If it's combined with the first one, the accuracy can even be enhanced. For the computational complexity, the first

one is least complex, the third one is the second least, while the second one has the most complexity. Therefore, according to the author's experiment results, the best method is to combine the first and third methods.

1.2.3 Advantages and Limitations of AE

One major advantage of AE based on above applications is that it can be performed at the interference in-service without any disturbance [15]. It also makes AE more advanced than other NDT since it is not necesssary to place the sensor right at the defect position. In addition, the localization ability gives another major advantage of AE. Therefore a suspected area can be reported to the client. This early warning advantage opens the way for performing following tests economically to verify the defect. Last but not least, AE provides a real-time monitoring method to the specimen.

The disadvantage of AE is that AE can only estimate qualitatively how much damage is in the material and approximately how long the components will last. Other NDT methods are still required for further examinations and provide quantitative results [14]. Another disadvantage is given by the fact that defects which are neither growing nor moving do not produce AE and can not be detected [16]. In addition, evaluation criteria are not existing in form of commonly accessible data, for example, the threshold of AE is set firmly to the knowledge and experience of the service provider. Also the background noise, both continuous and impulsive, makes AE signals less accurate [17]. High level of continuous noise such as fluid flow may obscure some weak AE signals. Some impulsive noise may produce acoustic signals similar to the genuine AE signals.

All in all, AE is a powerful and unique technique among all the NDT methods. It can be used to monitor the structure and provide early warning, but it also requires follow-up techniques to verify the defects. It plays an important role in real-time inspection, but it cannot detect a static defect as no elastic energy is rapidly released.

1.3 Characteristics of AE signals

The terminology of AE "signals" differs from "AE events". It is emphasized in this section to provide a transitional link between the AE testing part and signal analysis part.

The statistic signal parameters discussed in the last section are not enough for extracting the genuine feature of AE signals. Any acoustic sound may have a shape in time domain with acceptable statistic features similar to the shown one. Researchers begin to look into frequency domain for distinguished features of AE signals, as they realized only time domain information is not adequate to differentiate AE signals. Yoshida mentioned in [3] that the frequency characteristics of an AE signal has certain relationship with the external pressure and defect size of its releasing source. This is further explained as that higher pressure makes larger amplitude and higher frequency components, as well as larger defect produces larger amplitude and lower frequency components. However, such characteristics are still not enough to classify certain AE signals. This is because AE signals are non-stationary signals.

In the nature world, most acoustic signals are non-stationary, which means they are random transient signals whose statistic features, such as mean and variance, change over time. Therefore, time domain statistics only provide very rough outlook. Frequency analysis gives some information about a non-stationary signal. In fact, due to the time-varying factor, an analysis which is also time-changing is needed. The joint distribution combining both time domain and a transformed domain together, such as time-frequency and time-scale analysis, is introduced to appropriately process non-stationary signals with a much detailed scope.

Previous analysis using the same data base as this thesis but from different project showed that time-frequency analysis is a popular and important tool for AE signal processing. Students from Penn State University use STFT for analyzing. Another group from Arizona State University applied matching pursuit (MP) which is also a time-frequency method for the classification [18]. Calling for better resolution of the low frequency components in the provided AE signals, wavelet transform which is a time-scale analysis is more appropriate

for the data analysis and classification in this thesis.

1.4 Time-Frequency Analysis

1.4.1 Introduction to Time-Frequency Analysis

Time-frequency (TF) analysis is first introduced by Gabor in his "Theory of Communication", which states that any signal could be depicted as a superimposition of a large number of TF atoms [6]. These TF atoms, or basis functions, are defined as the localized part of a signal in both time and frequency domains. Therefore, TF analysis provides a joint distribution of time and frequency with the energy intensity at the atom location.

In TF distribution, signals are segmented into TF components inside the function space with each component having time, frequency, and energy (magnitude) information attached to it. This approach nicely fits the needs of non-stationary signals as all the three axis of time, frequency and energy are required to represent them efficiently and accurately [19].

A similar approach to TF distribution is Time-frequency representations (TFR) [20]. TFR characterizes a given signal over a time-frequency plane and yields more revealing information about the temporal localization of a signal's spectral components. TFR projects a one dimensional signal of $x(t)$ into a two dimensional function of time and frequency $TFR_x(t, f)$. The linear and quadratic time-frequency representations are the most commonly used TFR [21]. Spectrogram, which is the absolute value of STFT, is a fundamental example for linear TFR [20]. Wigner distribution (WD) is an instance for quadratic TFR.

1.4.2 Several Time-Frequency Decomposition Methods

Time-frequency localization can be achieved by first windowing the signal so as to cut off only a well-localized slice of $x(t)$ and then taking its Fourier Transform. This results in the STFT of $x(t)$, or Windowed Fourier Transform. The magnitude of the STFT is called the spectrogram. Since spectrogram has less resolution in the time-frequency plane, WD is introduced to give a better resolution for mono component signals. For multi component signals, WD introduces interferences between adjacent components in the time-frequency

plane. This interference is also called cross-component that oscillates in the time-frequency plane, and leads to a poor time-frequency representation of the multi component signals [20].

It is proposed in [22] and [23] that matching pursuit (MP) searches for a linear expansion approximating the signal $x(t)$, in terms of functions chosen from a complete and redundant set (dictionary). MP is an iterative algorithm. Rather than finding a global optimal expansion, it finds an optimal one-element expansion at each step of the operation. The rest of the one-element expansion will be expanded in the next iteration, and so forth. Mallat and Zhang in [22] use shifted and scaled Gaussian TF atoms as the basic dictionary elements to decompose a given signal into basic Gaussian atoms. They also accompanied the publication with a freely available software implementation [24]. The authors in [25] claimed that it is also possible to use more than one type of basic atom in the dictionary, and they developed a modified matching pursuit algorithm for classifying AE signals [18].

1.5 Time-Scale Analysis

1.5.1 Introduction to Wavelet Transform

Wavelet transform is the most recent solution to overcome the drawbacks of the Fourier transform. A wavelet is a kind of mathematical function targeted at dividing a given function or a continuous time signal into different frequency components, and studies each component with a resolution that matches its scale. In wavelet this is completed by shifting a scalable window along the signal and calculating the spectrum for each position. Then this process is repeated for needed times with a slightly shorter (or longer) window for each new loop. Finally, a collection of time-frequency representations of the signal at distinguished resolutions composes the output. As in wavelet, the details are not presented by frequency but by scale, wavelet analysis is also issued as time-scale analysis method.

Wavelet transforms are classified into discrete wavelet transforms (DWT) and continuous wavelet transforms (CWT). It should be noted that both DWT and CWT are of continuous time transforms. This means they can be used to represent continuous time signals. DWT use a specific subset of scale and translation values whereas CWT operate over every possible

scale and translation.

1.5.2 Advantages of Wavelet Transform over TF methods

Wavelet transforms have advantages over traditional Fourier transforms for representing functions that have discontinuities and sharp peaks, and for accurately deconstructing and reconstructing finite, non-periodic and/or non-stationary signals.

For all the TF methods, the common idea is how to cut the analyzed signal into time-frequency atoms and analyze these atoms separately. This method provides more information about the "when" and "where" of different frequency components in a signal [26], and all the TF methods just differ from each other in its way of cutting the signal. Here cutting the signal corresponds to a convolution between the signal and the cutting function such as the window in STFT. However, as stated by the Heisenberg uncertainty principle, it is impossible to identify the exact frequency and the exact time of occurrence of this frequency in a signal. In another word, the time resolution and frequency resolution can not be simultaneously increased. Thus, a signal can not be denoted in the form of infinite points in the time-frequency plane.

MP is an advanced TF method as it is not normally restricted by the uncertainty principle. In fact, MP is similar to wavelet transform in a certain way that both of them are calculated iteratively, and both of them defined a framework in which one can insert a function to decompose the signal. In MP this comes as a dictionary form requiring basic atoms, and in wavelet this is a transform operated with defined wavelets (mother wavelets). However, the later one is still more advanced than the former. The iterative requirements for wavelet can be solved with fast Fourier transform (FFT) inside one computation. This is because each iteration in wavelet is independent with others. While for MP, each iteration is based on the previous one. Therefore wavelet is much faster than MP computationally. In addition, the dictionary of MP is not well established as wavelet transform. A common used basic atom in MP is the Gaussian atom. While for wavelet transform, many mother wavelets are issued, both orthogonal and non-orthogonal. All in all, MP is a further de-

velopment among TF methods, while wavelet creates a new frame and direction, time-scale analysis, which provides better resolution for signal analysis with higher efficiency.

1.6 Proposed Work and Motivation

The main purpose of this thesis is to design automatic classifiers to avoid the arduous and tedious manual classification works. Report from industry shows that less than one percent of the recorded signals are genuine AE signals. Thus it is desirable to have an automatic classification program which should be able to work efficiently and accurately.

As this thesis is based on an industrial collaboration of pipe AE events inspection (will be thoroughly discussed in chapters 3 and 4), the finalized work will be a combination of software and hardware development. If possible, the auto classifier will be part of the hardware to filter noise and save the storage of recording. Also the parameters are designed to be controllable over wireless network in the end product. Therefore, it is very important that the algorithm for auto classifier should be of high accuracy and efficiency, as well as feasible for embedded hardware implementation.

TF methods are generally used in the industry according to the provided information. Previous works showed that STFT and MP analysis have been developed for the pipe AE events inspection. In addition, the analysts not only look into these visual distributions, but also listen to the AE signals. This means, although the AE signal covers a range of 8 kHz to 40 kHz (the boundary is limited by the sensors), analysts can differentiate real AE signals just according to the hearable frequency band - lower than 20 kHz. In another word, AE signals greatly varied from other sounds in low frequency ranges.

Considering all the above factors, the wavelet transform is chosen in this thesis for the design of auto classifier. Its inherent multi-resolution characteristic provides excellent resolution for low frequency components. It perfectly suits our objective of enlarge the low frequency parts and shrink the high frequency parts of AE signals. While TF methods only have constant resolution over the whole time-frequency plane. Moreover, not many scales are required in this work as we just need to focus on low frequency part of the provided

signals. Thus wavelet is computationally faster then previous TF analysis.

In this thesis work, both wavelet transform and STFT are applied to compare the results and verify the advantage of wavelet analysis. After the comparison, auto classifiers are built up for programming. And then the program is tested over two industrial projects to examine its workability.

1.7 Thesis Contribution and Outline

1.7.1 Contribution

As developed for industrial application, the contribution of this thesis work can be summarized as the following:

1. This thesis verifies the advantages of time-scale analysis in processing non-stationary signals over TF methods. As discussed in section 1.3 and will be further proven in Chapter 2, AE signals are such type of non-stationary signals. Compared with STFT and MP techniques used for the same objective - AE signal detection, it is demonstrated in this thesis that wavelet transform has better precision than STFT and greater efficiency than MP.

2. Although wavelet transform has been well applied in many fields such as image processing, bioengineering and medicine fields, it is a new and specific approach to apply wavelet analysis in AE monitoring in pipeline. This thesis integrates modern signal processing methods and mechanical testing techniques together, and yields a feasible and extendable product for the industry. In addition, a journal paper is to be published based on the thesis work [27] as well as a conference paper [28].

3. The algorithm and program developed in this thesis are proven to be robust compared with the company's previous analyzing techniques. The auto classifier developed based on the algorithm in this thesis are tested over large quantity of signals. The experiment results turn to be considerable which show that the efficiency of the whole testing procedure has been greatly enhanced.

4. In addition, as the auto classifiers are adaptive and designable for various conditions, they provided a framework which is capable for different types of industrial projects. Moreover, the auto classifiers are easily understood and customized, which are friendly to analysts.

1.7.2 Thesis Outline

The remaining of this thesis is organized into five chapters as the following:

- Chapter 2 provides the basis of wavelet transform and STFT. It explains in detail the methodologies and techniques employed in this study. The calculation flow and main codes are provided.

- Chapter 3 gives the physical condition and environment for this AE signal detection work, as well as previous extracted features in time-frequency plane. Then the auto classifiers are defined, and the parameters for designed program are illustrated.

- Chapter 4 documents the application of the proposed methods in two industrial projects, and provides the experiment results.

- Chapter 5 provides the conclusion and future works for this thesis.

Chapter 2

Methodologies

2.1 Introduction

In industry, AE testing is conducted to detect defects in pipelines as detailedly described in the following section. Then these collected AE signals need to be further processed so as to extract their features and establish an automatical algorithm to further detect them. After introducing to the current applied technology, the methodologies of STFT and wavelet transform are elaborated and compared in this chapter. In addition, several mother wavelets are provided to form a thorough view of wavelet, and the key parameters are discussed in the last part of this chapter.

2.2 Current Applied Technologies in industry

2.2.1 Introduction to the Physical Conditions

AE Signals from the pipelines provide the observed data for this research. The environment and preconditions are described below.

All the tested portions are Lined Cylinder Pre-stressed Concrete Cylinder Pipe (PCCP) [29], as shown in Fig. 2.1. The PCCP is constructed by first casting a steel cylinder outside of a concrete core, and then the core is reinforced by wrapping pre-stressed wire around it. This high strength wire is designed to force the core tighter, and is then coated with a mortar coating, so as to provide corrosion protection to the wire. Therefore, this pre-stressing wire is

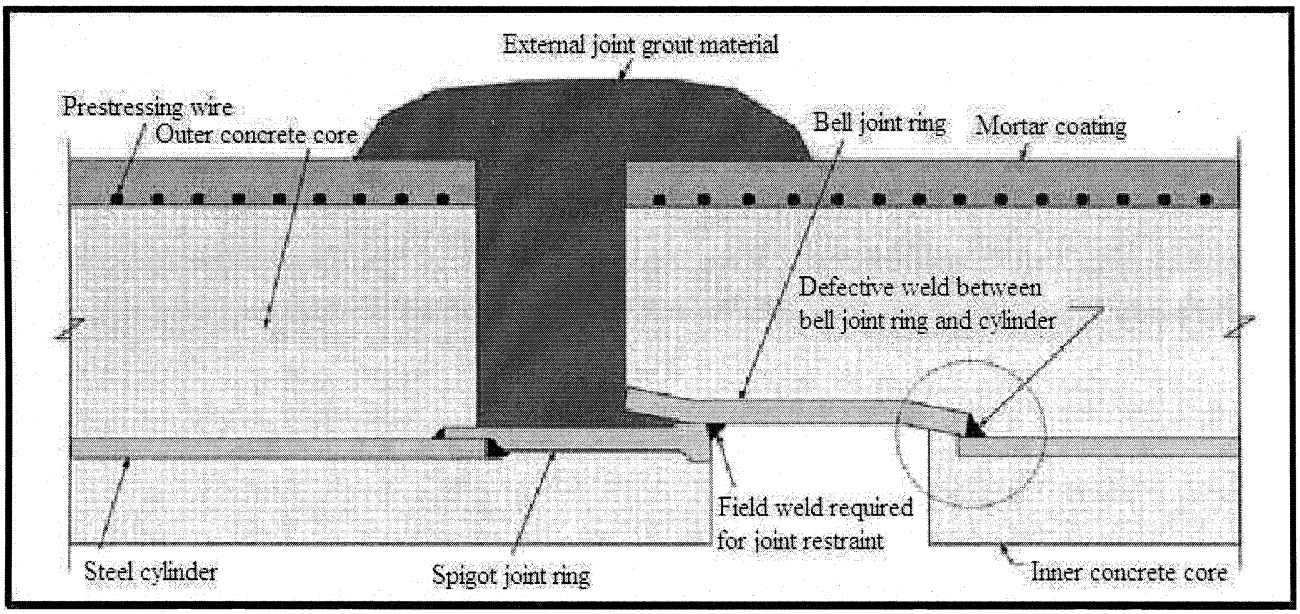

Figure 2.1: Lined cylinder PCCP.

the key component of the PCCP, and the main purpose of AE testing is to take precautions against the corrosion and breakage of the wire.

Once the wire break or split occurs, the tension energy embedded in the wires will be released, and acoustic waves will be generated. After propagating through the medium inside the pipe, these waves can be detected and recorded by acoustic sensors as long as the amplitude of the signal is higher than the pre-defined threshold. These recorded acoustic signals are defined as wire-related events(WRE) in industry, and the AE testing is conducted to detect WRE signals in PCCP.

In current practice, two types of sensors have been used to detect WRE signals: hydrophone and accelerometer. Hydrophones are constructed of ceramic materials and can detect acoustic signals by sensing the vibration that propagates through water. Hydrophones are installed through valves into the water column inside the pipeline, as shown in Fig. 2.2(a). Accelerometers are installed on the surface of the pipeline, as shown in Fig. 2.2(b). Incentive to use accelerometers in AE testing is to assist hydrophones, as hydrophones are more

sensitive than accelerometers. They are also used in empty pipelines, where hydrophones do not work.

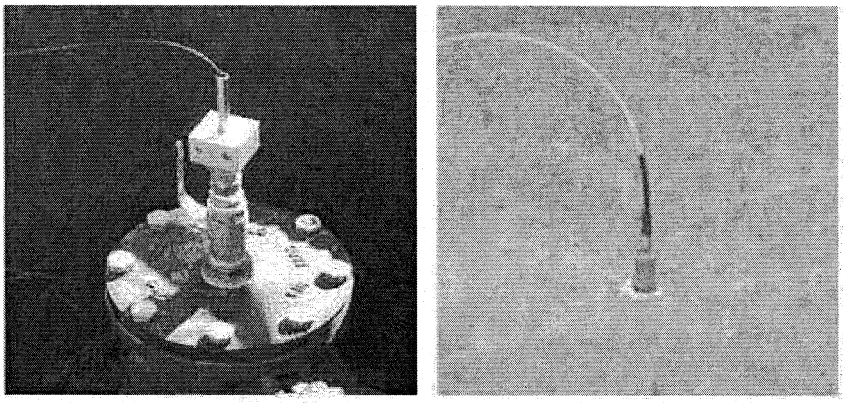

Figure 2.2: (a): A hydrophone sensor. (b): An accelerometer sensor.

Once the AE event occurs, the signal will propagate both ways along the pipeline, and may be detected by the closest pair of sensors. Sometimes if the amplitude is large enough, the signal might be detected by the third or the fourth sensor. As studied in [1], the detected result is reliable with sensor spacing at 262 meters distance, and this can vary according to landscape, temperature, pipe structure, etc. Therefore, an ideal WRE signal should be detected by two sensors closest to it, and the arrival time difference can be used to localize the position of the defect [1].

2.2.2 Introduction to the Industrial Analysis Technique

The STFT software is used in the data analysis in industry. The following example shows the analyzing method and judging standard that is used.

Fig. 2.3 is an example of AE signal detected by the closest two sites: the sensor used in site 1 is a hydrophone, so it is represented as a white square drilling across the pipe wall; the sensor used in site 2 is an accelerometer, and it is expressed as a square mounted on the surface of the pipe wall. The analysis result shows that site 1 is 68.6 meters from the event

[1]If the signal is only picked up by one sensor, then the position cannot be accurately localized, and the recorded data will not be considered as useful.

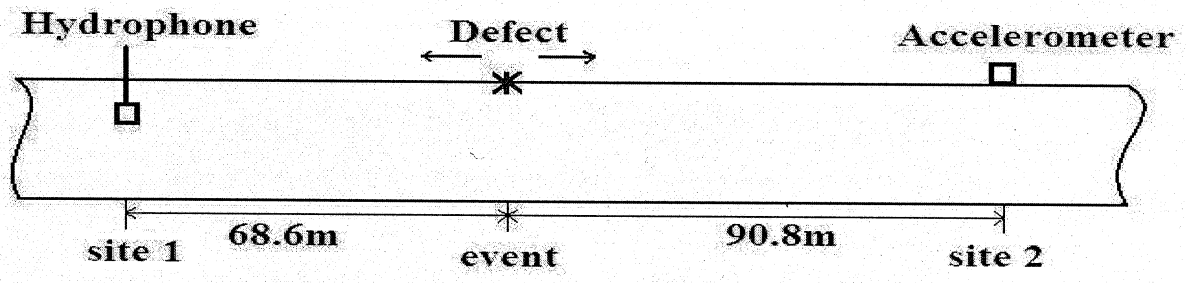

Figure 2.3: An AE event detected by two sites.

and site 2 is 90.8 meters from the event. Some features of this WRE signal resulted from the STFT software are shown in Fig. 2.4. Figs. 2.4(a), 2.4(c), and 2.4(e) show the time domain, frequency domain and the Gabor time-frequency domain respectively, of the recorded signal at site 1; Figs. 2.4(b), 2.4(d), and 2.4(f) provide the corresponding information of the recorded signal at site 2 [4].

Figs. 2.4(a) and 2.4(b) clearly show that the signal amplitude recorded by the hydrophone is much larger than that recorded by the accelerometer. In the Gabor transform, Figs. 2.4(e) and 2.4(f), larger amplitude and energy intensity in the signal will result in a darker color. From the time-frequency analysis shown in Figs. 2.4(e) and 2.4(f), the signal-to-noise ratio (SNR) of the signal detected by the hydrophone is much higher than that detected by the accelerometer, on account of a greater energy of the left signal. Although the noise level of these two signals are almost the same (shown as the gray level of the background), the larger energy in the left signal results in a larger SNR.

Some observations can be drawn as follows:

- In the time domain [Figs. 2.4(a), 2.4(b)]:

The duration of the signal is usually less than 0.05 seconds. The intensity of the signal should be much larger than the background. while in frequency domain (Figs. 2.4(c), 2.4(d)) this corresponds to the spectrum amplitude of the signal, and in the time-frequency Gabor window (Figs. 2.4(e), 2.4(f)) it means the color of the signal should be much darker than the background.

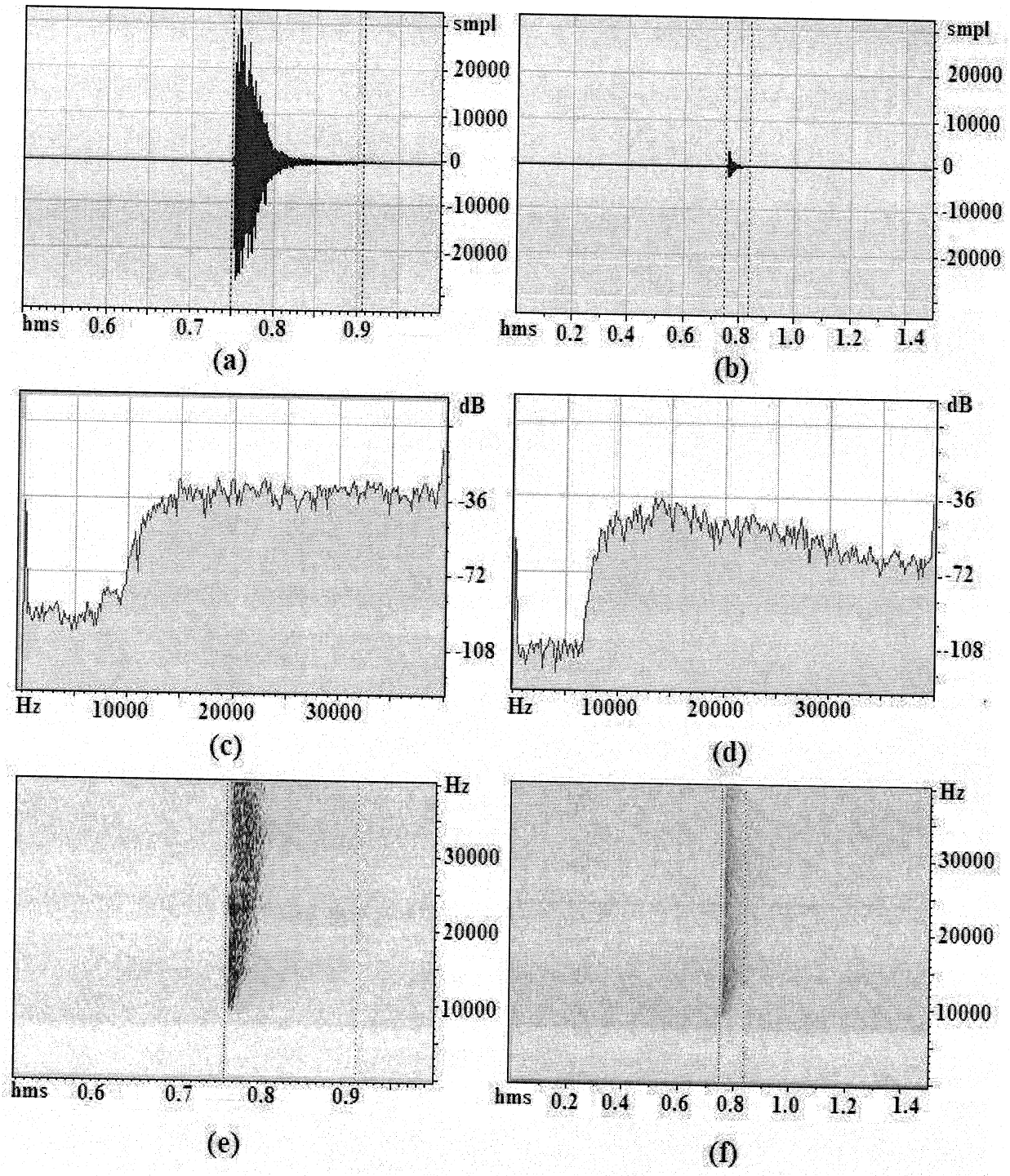

Figure 2.4: (a), (c) and (e): The time domain, frequency domain, and Gabor transform, respectively, of the signal recorded by an hydrophone. (b), (d) and (f): The same signal recorded by an accelerometer.

- In the frequency domain [Figs. 2.4(c), 2.4(d)]:

These figures show the "real-time" [2] spectrum of the signal. This WRE signal has the following unit step form, as shown in Fig. 2.5(a), where the solid line is the spectral shape at the beginning time , and the dashed line is the spectral shape at the ending time.

For the beginning of the signal in time axis: 7 kHz is the start frequency of all sounds (mostly background), 12 kHz is the start frequency of the WRE signal, and the highest frequency is above 40 kHz.

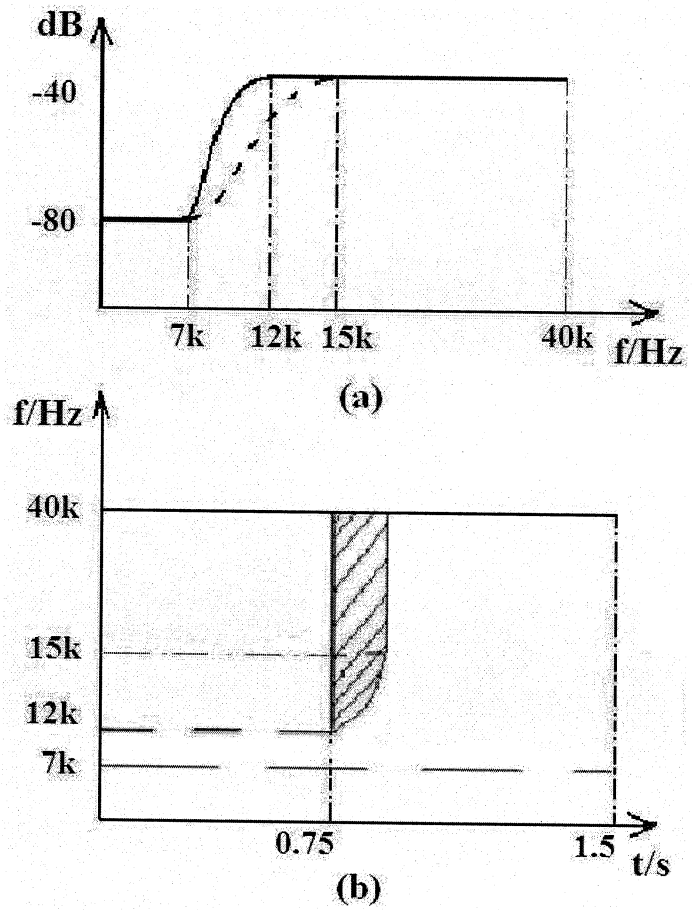

Figure 2.5: (a): Frequency response of an WRE signal: solid line is the spectral shape at the beginning time; dashed line is the spectral shape at the ending time. (b): Gabor windowed time-frequency distribution of an WRE signal.

[2]The quotation mark is used because this spectrum is not instantaneous but a windowed spectrum which changes with time.

For the ending of the signal in time axis: 15 kHz is the start frequency of WRE signal, the highest is above 40 kHz. These parameters can be different in particular situations, while the shape should be similar. As shown in Figs. 2.4(c) and 2.4(d), the high frequency decrease greatly due to the attenuation of signal propagating through the pipeline to the accelerometers.

- In the time-frequency Gabor window [Figs. 2.4(e), 2.4(f)]:

As shown in those Gabor figures, the power density starts at above 7 kHz, while lower than 7 kHz it is all white, which means that there is no frequency component in this part. From the beginning of the signal at 0.75 seconds until the ending at 0.80 seconds, the shape of the power density is like a vertical downward knife, as shown in Fig. 2.5(b). The peak of the knife is the beginning of the signal with 12 kHz frequency, which decreases earliest and at the fastest speed; hence, at the ending time, 15 kHz becomes the start frequency. In addition, the intensity of the signal from 15 kHz to 40 kHz is almost uniformly distributed, and this feature makes the two vertical parallel lines.

2.3 Basis of STFT

2.3.1 Computation of STFT

Fourier transform is defined to obtain the frequency distribution of a signal only in the case that the signal is transformed through the whole time domain. In addition, the stationarity of the signal is required. In another word, the spectrum information of the signal has been averaged through the whole time domain, which results in the loss of real-time spectrum occurrence [30].

Short-Time Fourier Transform (STFT) was introduced by Gabor [6] to compensate the limitation of classical Fourier Transform, which provides an original joint time-frequency method. It uses a measuring window to restrict the Fourier transform in a limited time range and then obtain the spectrum on this time range. As Fig. 2.6(a) shows, this real and symmetric window $g(t)$ is delayed by u on time domain, and modulated by the frequency

ξ [31]:

$$g_{u,\xi}(t) = e^{i\xi t} g(t-u) \tag{2.1}$$

The STFT of a signal $f(t) \in L^2(\mathcal{R})$ is:

$$Sf(u,\xi) = < f, g_{u,\xi} > = \int_{-\infty}^{\infty} f(t) g(t-u) e^{-i\xi t} dt \tag{2.2}$$

where S stands for applying STFT to $f(t)$ with the (u,ξ) window, $< f, g_{u,\xi} >$is the inner product of $f(t)$ and $g_{u,\xi}(t)$, and $L^2(\mathcal{R})$ is the whole function space. Therefore, the multiplication by $g(t-u)$ localizes the Fourier integral of $f(t)$ in the neighborhood of $t = u$, as shown in Fig. 2.6(a). In the figure, (u,ξ) is the center of the window in time-frequency domain, while σ_t and σ_ω are the width and length of the window, respectively. Therefore, after taking STFT, the energy of $f(t)$ is spread over both time interval $[u - \sigma_t/2, u + \sigma_t/2]$ and frequency interval $[\xi - \sigma_\omega/2, \xi + \sigma_\omega/2]$.

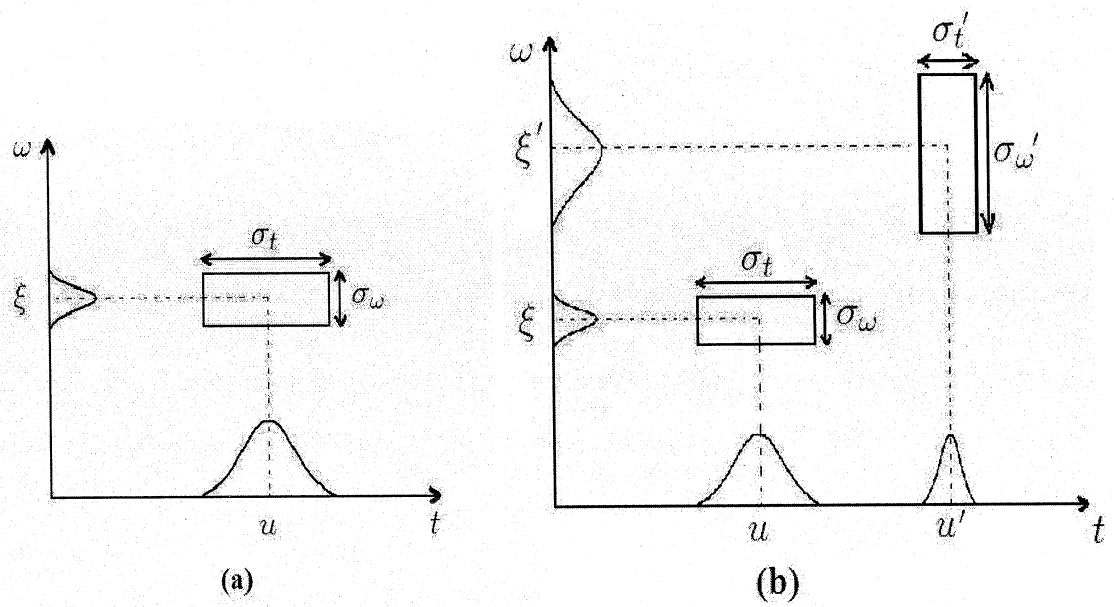

Figure 2.6: (a):The STFT window. (b): The Heisenberg principle of certain precison.

However, according to Heisenberg uncertainty principle, the limitation of this time-frequency plane localization is:

$$\sigma_t \sigma_\omega \geq 0.5 \tag{2.3}$$

where σ_t, σ_ω corresponding to the time and frequency atom length, and $\sigma_t\sigma_\omega$ is the area. This means, the time and frequency atom cannot be simultaneously small, thus the details are both averaged through time and frequency domain inside the window. As Fig. 2.6(b) shows, the window at (u, ξ) integrate over $[u - \sigma_t/2, u + \sigma_t/2]$, and generate the frequency atom with length σ_ω. And the other window at (u', ξ') has a smaller time integral σ'_t, which generates a bigger frequency atom with length σ'_ω. Therefore, STFT can only give a certain resolution, which is not high enough to show the detailed interaction of time and frequency.

2.3.2 Disadvantages of STFT

As discussed by Kaiser [32], STFT provides an inaccurate and inefficient method of time-frequency plane analysis, as it imposes a scale to do the localization. First, the inaccuracy comes from the aliasing of high and low frequency components, which actually do not fall into the frequency of the window [33]. Secondly, several window lengths must be selected and applied to determine the most appropriate one. Due to Heisenberg uncertainty principle, even though the appropriate window size has been determined, the provided time-frequency analysis is not only single resolution, but always averaged on both time and frequency dimensions.

STFT does not change the fact that the information in this time-frequency box is still averaged over both time and frequency sides and that the information of sudden changes is lost. Concerning this essential issue of obtaining the occurrence of time-frequency information, wavelet transform is introduced to perform this time-frequency-scale transformation, aiming at combining amplitude and spectrum decomposition together and as accurately as possible. In principle, when applied to the detection of discontinuities, short time phenomenon, and abrupt changes in a signal, Wavelet transform has better performance than other signal processing methods. It also provides higher resolution and better precision in presenting real-time changes of a signal's spectrum density function, thus, it is an essential way to characterize time-frequency structures [6].

2.4 Basis of Wavelet Transform

Wavelet transform can be used to analyze non-stationary signal via decomposing and reconstructing them with wavelet basis or wavelet functions. There are two types of wavelet transform: Continuous Wavelet transform (CWT) and Discrete Wavelet transform (DWT).

The term "wavelet basis" usually refers to orthogonal wavelets in the Hilbert space, while "wavelet function" generally represents either orthogonal or non-orthogonal wavelets [34]. In DWT, orthogonal wavelet basis is often applied to give the most compact representation of the signal. However, for time series analysis, CWT with non-orthogonal wavelet functions are recommended as it is highly redundant at large scales, and the wavelet spectrum is highly correlated [33]. In the proposed algorithm, CWT is also selected to apply the time-scale analysis for the time domain acoustic signals.

2.4.1 Continuous Wavelet Transform

In CWT, a signal with finite energy is projected on a continuous collection of frequency bands, which compose the whole function space $L^2(\mathcal{R})$. For example, we can take every frequency band of the form $\left[\frac{f}{2}, f\right]$, for all positive f of the signal. Thus, the original signal can be reconstructed as an appropriate integration over all the wavelet transformed frequency components.

The wavelet functions are the scaled shifts of one generating function $\psi_0(t) \in L^2(\mathcal{R})$, which is a continuous function in both the time domain and the frequency domain called the mother wavelet. For instance, with $\psi_0(t) = \sin(t)$ as mother wavelet, at frequency band $[1, 2]$, and scale at 1, the wavelet function is: $\psi(t) = 2\sin(2t) - \sin(t)$. If the scale parameter is a, the frequency band becomes $\left[\frac{1}{a}, \frac{2}{a}\right]$, then the general wavelet functions are given as:

$$\psi(t) = \frac{1}{\sqrt{a}}\psi_0\left(\frac{t-b}{a}\right) \tag{2.4}$$

where a is a positive scale factor and b can be any real number that defines the shift. The normalization factor $\frac{1}{\sqrt{a}}$ is introduced to ensure the wavelet function have unit energy at each sale a.

CWT uses these wavelet functions to transfer time series into a time-scale wavelet domain, which provides a very detailed localization on both time t and scale a directions. Mathematically, it is defined as the convolution of the signal $f(t)$ with chosen wavelet functions [26]:

$$W_f(a,b) = \frac{1}{\sqrt{a}} \int_{-\infty}^{\infty} f(t)\psi_0^* \left(\frac{t-b}{a} \right) dt \tag{2.5}$$

where W_f represents the wavelet transform of $f(t)$, and '$*$' denotes the complex conjugation operation. Valens also emphasized in his article [26] that it is important the wavelet functions are not specified in this mathematical wavelet frame, which is a clear ridge between wavelet transform and other transforms including Fourier transform. It is essential that wavelet transform designed a framework in which one can design wavelets for their own properties.

There are several known mother wavelets such as Morlet and Mexico hat wavelet, and all the mother wavelets must satisfy the conditions of zero mean and unit energy:

$$\begin{aligned} \int_{-\infty}^{\infty} \psi(t)dt &= 0 \\ \int_{-\infty}^{\infty} |\psi(t)|^2 dt &= 1 \end{aligned} \tag{2.6}$$

2.4.2 Discrete Wavelet Transform

As computing all the wavelet coefficients is quite time consuming, DWT is developed to simplify the computing work. It picks a discrete subset of the coefficients to reconstruct the signal. The Haar wavelet is the simplest wavelet in DWT to illustrate how wavelet decomposition works [35].

Fig.s 2.7(a) and 2.7(b) are the non-scaled Haar mother and child wavelets, respectively . They are given as:

$$\begin{aligned} \phi(t) &= \{ \begin{array}{ll} 1, & 0 \leq x < 1 \\ 0, & else \end{array} \\ \psi(t) &= \phi(2t) - \phi(2t-1) \end{aligned} \tag{2.7}$$

These two non-scaled wavelets can be labeled as ϕ_0 and ψ_0. If we choose $a = 2$ as the scale factor, then at scale 1, the ϕ_1 window will be 2^{-1} length, and this can be obtained by

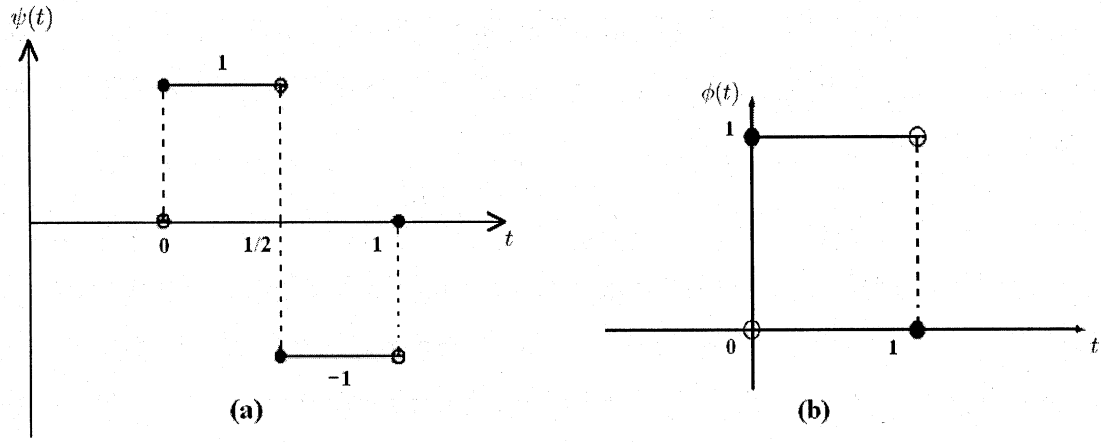

Figure 2.7: (a):Mother wavelet of Haar. (b): Child wavelet of Haar.

$\phi_1 = \phi_0 \oplus \psi_0$, where $\oplus$ donates orthogonal intersection, and ψ_0 is the orthogonal complement of ϕ_0 in ϕ_1. Analogically, a smaller window ϕ_2 with 2^{-2} can be generated as: $\phi_2 = \phi_1 \oplus \psi_1 = \phi_0 \oplus \psi_0 \oplus \psi_1$. Therefore, if we want a window ϕ_j that is small enough to represent every point of the signal, it can be generated as:

$$\phi_j = \phi_{j-1} \bigoplus \psi_{j-1} = \phi_{j-2} \bigoplus \psi_{j-2} \bigoplus \psi_{j-1} = ... = \phi_0 \bigoplus \psi_0 \bigoplus \psi_1 \bigoplus \psi_2 \bigoplus ... \bigoplus \psi_{j-1} \quad (2.8)$$

This means, every finite-energy signal can be decomposed by a wavelet at any scale level j. With this technique, the decomposed signal can easily be analyzed and reconstructed. Fig. 2.8 is an example that shows part of the decomposition procedure. Fig.s 2.8(a) is the original signal with two impulse noises, 2.8(b) and 2.8(c) are the ϕ_4 and ϕ_7 decomposition of the signal. It is shown that large scale contains more basic information like ϕ_4, and small scale records more detailed information like ϕ_7. Therefore, if the signal is reconstructed using only useful scales, the noise can be omitted.

Compared with CWT, DWT is easier to compute. However, as DWT is discontinuous, those decomposed signals contain less information in each scale, which means more scales are needed in the reconstruction of the whole signal.

Sequently, CWT is a better choice in this AE detecting application. The Morlet wavelet is selected as the mother wavelet, which is a complex continuous wavelet.

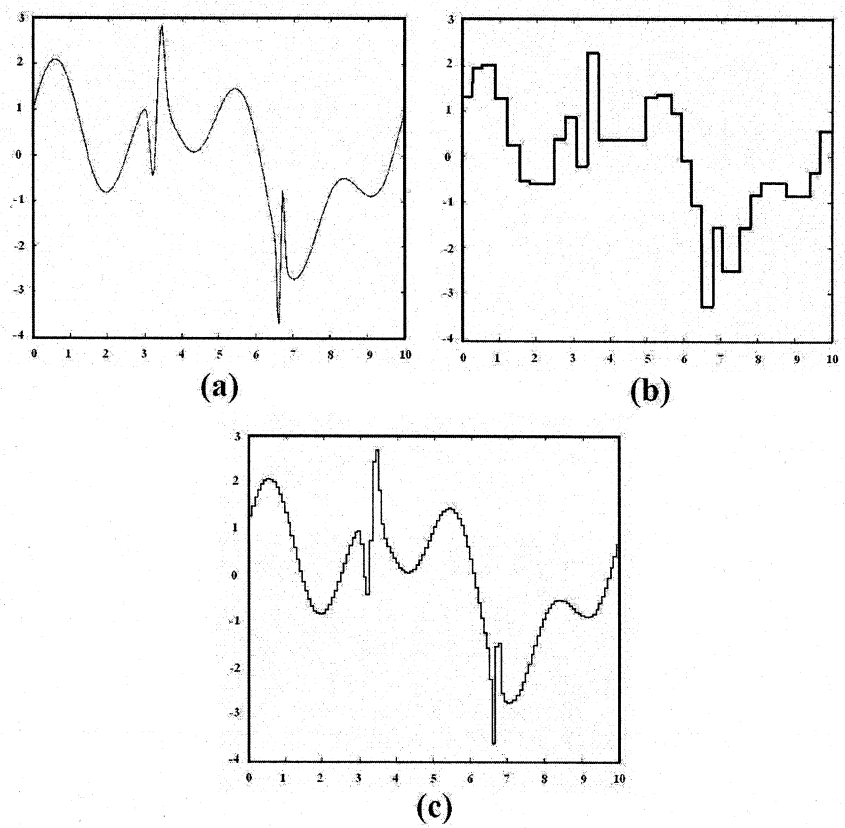

Figure 2.8: (a): The original signal. (b): ϕ_4 of the signal.(c): ϕ_7 of the signal

2.5 Comparison of Wavelet Transform with STFT

Compare equation (2.5) with continuous Fourier transform:

$$F_f(\omega) = \int_{-\infty}^{\infty} f(t)e^{-j\omega t}dt \tag{2.9}$$

one can easily figure out that Fourier transform is a specialized form of wavelet by substituting the wavelet functions with infinite and periodical sine and cosine waves. The waves are infinite, thus there is no shift. This finally results in the non-localizable of Fourier transform in time domain. If we only take the wave in one period as the wavelet function (similar to what STFT does), then the period can be considered as the scale factor, as both of these two methods are sampling and quantizing signals so as to decompose them. As "period" in Fourier transform and "scale" in wavelet transform are proportional, frequency and scale are inversely proportional to each other. That is, high frequency components refer to small scales in wavelet domain, and both of them represent small details in the signal.

When facing the non-localizable problem of Fourier transform, researchers introduced STFT to impose the localization grid onto the signal. Unfortunately, this method leads to a confusing way of explaining frequency components in the time-frequency domain, as we discussed at the very beginning of this section. The particular window in STFT is a scale factor. However, if its size is constant, it can only represent the averaged frequency components inside the window, but not the real frequency components. This is why Kaiser regards it as inaccurate in building up the time-frequency analysis [32].

Therefore, compared to regarding wavelet transform as an extension of Fourier transform, it is more appropriate to state that Fourier transform is a particular case of wavelet transform, as wavelet transform is not only a transform but a framework for researchers to fill in their own wishes.

2.5.1 Scale vs. Frequency

When comparing wavelet transform with Fourier transform, it should be noted that frequency in Fourier transform and scale in wavelet transform are inversely proportional to each other.

Hence, scale has a certain relationship with frequency. In [36], the following equation states this relationship:

$$a = \frac{b}{\omega} \tag{2.10}$$

where b is a constant, a is the scale parameter, and ω is the circular frequency of the signal.

2.5.2 Multi-resolution vs. Single Resolution

Wavelet transform has multi-resolution for different scales. Generally speaking, it provides excellent resolution in the large scale part which corresponds to the low frequency region. While for small scale part, it has acceptable resolution regarding the computational complexity issue. In practical aspect, wavelet transform enhances the low frequency components and compresses the high frequency details. Actually these compressing and enhancing properties make Wavelet transform more advanced than Fourier transforms such as STFT. This property meets the need of our research appropriately. While for STFT, there is only one consistent resolution for the whole signal in time-frequency plane, thus the resolution of those frequency components cannot be distinguished for different uses. In this AE application, we need to both enlarge low frequency components and compress high frequency components as claimed in Chapter 1. These two objectives can be easily achieved using Wavelet transform rather than STFT. Because in STFT, different frequency components will be enlarged or shrunk together, as it has only one consistent resolution.

2.5.3 Detailed Exhibition vs. Averaged Displacement

Except for above facts, the resolution of using STFT in AE signal processing is too low, and the details of the signal are wholly averaged over the STFT window. This means, if we want smaller unit length and more details in the frequency domain, the unit length in the time domain will be increased as the area of this time-frequency piece should keep the same. While for wavelet transform technique, the problem has been solved, as it is designed to exhibit the sharp discontinuities and fast changes.

2.6 Computer Implementation of CWT

2.6.1 CWT Applied to Discrete Time Sequence

Computation of CWT

Although CWT has been chosen for the time series analysis in this thesis, a discrete form of CWT is needed for discrete time sequence and for the computational implementation. We can make the assumption of a time sequence, $x(n)$, with equal time step Δ_t [3] and $n = 0, 1, \cdots, N-1$. Assume the wavelet function is given as $\psi_0(t)$, where t is a non-dimensional time parameter to form the function. Take Morlet wavelet for example (details are provided in section 2.6.3):

$$\psi_0(t) = \pi^{-\frac{1}{4}} e^{j\omega_0 t} e^{-\frac{t^2}{2}} \tag{2.11}$$

This is a complex sine wave modulated by a Gaussian function, and ω_0 donates the non-dimensional frequency parameter. Then wavelet transform in (2.5) can be written as [33]:

$$W_f(a,b) = \sqrt{\frac{\Delta_t}{a}} \sum_{n=0}^{N-1} \left\{ x(n) \psi_0^* \left[\frac{(n-b)\Delta_t}{a} \right] \right\} \tag{2.12}$$

In this equation, it can be seen that the convolution should be done for N times for each scale a. Thus, we can use discrete Fourier transform (DFT) to complete these N times convolution simultaneously. The DFT is calculated as:

$$\hat{X}_k = \frac{1}{N} \sum_{n=0}^{N-1} x(n) e^{-\frac{2\pi j k n}{N}} \tag{2.13}$$

where ' ^ ' donates the DFT of the term beneath the hat. According to Fourier's properties, convolution in time domain corresponds to multiplication in frequency domain. Hence equation (2.12) can be written as:

$$W_f(a,b) = FFT^{-1} \left\{ \sqrt{\frac{2\pi a}{\Delta_t}} \left[\hat{X}_k \hat{\Psi}_0{}^*(a\omega_k) e^{i\omega_k b \Delta_t} \right] \right\} \tag{2.14}$$

[3] In Cavlens' paper [33] this is δ_t. However, here we think it would be better to use Δt to represent the time step.

where $\hat{\Psi_0}^*(a\omega_k)$ donates the Fourier transform of the term $\psi_0^*\left[\frac{n\Delta_t}{a}\right]$, and ω_k is the angular frequency defined as:

$$\omega_k = \begin{cases} \frac{2\pi k}{N\Delta_t}, & k \leq \frac{N}{2} \\ -\frac{2\pi k}{N\Delta_t}, & k > \frac{N}{2} \end{cases} \tag{2.15}$$

Reconstruction of CWT

After manipulating the CWT of a signal such as denoising, the decomposed signal may need to be reconstructed for the coming processing. Although the reconstruction technique is not applied in this thesis, a brief calculation procedure should be provided here for the completeness of the wavelet transform theory.

Consecutively, CWT is computed as the inverse Fourier transform of the two sequences as shown in equation (2.14), which means the Fourier transform of $W_f(a,b)$ is:

$$\hat{W}_f(a,b) = \sqrt{\frac{2\pi a}{\Delta_t}}\left[\hat{X}_k\hat{\Psi_0}^*(a\omega_k)e^{i\omega_k b\Delta_t}\right] \tag{2.16}$$

As we know that the given wavelet function $\psi_0(n)$ should satisfy the principle of zero mean and unit energy, which mathematically means:

$$\sum_{n=0}^{N-1}\psi_0(n)\psi_0^*(n) = 1 \tag{2.17}$$

Multiply both sides of equation (2.16) with $\sqrt{\frac{\Delta_t}{2\pi a}}\hat{\Psi}_0(a\omega_k)e^{-i\omega_k b\Delta_t}$, Then the new right side will remain the Fourier transform of the time sequence $x(n)$. And the new left hand will become: $\sqrt{\frac{\Delta_t}{2\pi a}}\hat{W}_f(a,b)\hat{\Psi}_0(a\omega_k)e^{-i\omega_k b\Delta_t}$. Therefore $x(n)$ can be reconstructed with applying inverse Fourier transform to this new left term.

2.6.2 Matlab Implementation of CWT

Decomposition

The wavelet transform is implemented using matlab, using the terms provided in [36]. In the book, equation (2.16) is written as the following [4] :

$$L_\psi f(a,t) = FFT^{-1}\left[\sqrt{\frac{2\pi}{a}}\hat{\Psi}_a(\omega)\hat{f}(\omega)\right] \tag{2.18}$$

where $\hat{\psi}_a(\omega)$ donates $\hat{\psi}(-a\omega)$ corresponding to the following replacement [5] :

$$\psi_a(t) = \psi^*(\frac{-t}{a}) \tag{2.19}$$

Also in equation (2.18), the $L_\psi f(a,t)$ defines the wavelet transform of $f(t)$ with $\psi(t)$ as the given wavelet function and 'a' as the scale factor.

Therefore, the fast algorithm for the computation of $L_\psi f(a,t)$ leads to the following steps [36]:

1. Define the sequence $\{\psi_a(kT_s)\}_{k=0}^{N-1}$, where ψ_a is defined in equation (2.19).
2. Compute the FFT of this sequence with the result of a sequence $\{A_k\}_{k=0}^{N-1}$.
3. Compute the FFT of the time sequence $\{f(kT_s)\}_{k=0}^{N-1}$ resulting in $\{F_k\}_{k=0}^{N-1}$.
4. Apply the IFFT to the produced sequence $\sqrt{\frac{2\pi}{a}}\{F_kA_k\}_{k=0}^{N-1}$ to obtain the wavelet distribution $\{L_\psi f(a,kT_s)\}_{k=0}^{N-1}$.

Table 2.1 gives a frame of the above algorithm Schematically. It should be noted that this algorithm can be applied to any positive scale factor. Theocratically negative scale factor also can be used, while positive numbers is for practical implementation. Usually one takes $a = T_s, 2T_s, ..., (N-1)T_s$ considering the sampling issue.

[4] This equation refers to equation (2.21) in [36]
[5] This equation refers to equation (2.20) in [36]

$$\boxed{\begin{array}{c} \{\psi_a(kT_s)\}_{k=0}^{N-1} \rightarrow \{A_k\}_{k=0}^{N-1} \\ \Downarrow \\ \{f(kT_s)\}_{k=0}^{N-1} \rightarrow \{F_k\}_{k=0}^{N-1} \\ \Downarrow \\ \sqrt{\frac{2\pi}{a}}\{F_k A_k\}_{k=0}^{N-1} \leftarrow \{L_\psi f(a, kT_s)\}_{k=0}^{N-1} \end{array}}$$

Table 2.1: Flow of the computation for $L_\psi f(a,t)$: $\rightarrow$ and $\leftarrow$ donates FFT and IFFT, respectively.

Reconstruction

For the reconstruction of a wavelet transformed signal, the fast algorithm is given as [36]:

1. Compute the FFT of sequence $\{\psi_a(kT_s)\}_{k=0}^{N-1}$ donated with $\{A_k\}_{k=0}^{N-1}$.

2. Compute the FFT of sequence $\{\text{Ł}_\psi(a, kT_s)\}_{k=0}^{N-1}$ donated with $\{B_k\}_{k=0}^{N-1}$.

3. Compute the sequence $\{F_k\}_{k=0}^{N-1}$ given:

$$F_k = \sqrt{\frac{a}{2\pi}}\frac{B_k}{A_k} \tag{2.20}$$

4. Apply the IFFT to this produced sequence F_k to retrieval the time sequence $\{f(kT_s)\}_{k=0}^{N-1}$.

Note that equation (2.20) requires A_k to be nonzero for all k. If this is not satisfied, steps 1 to 3 will be repeated for suitable values of a, which may result in a completely recovery of $\{F_k\}_{k=0}^{N-1}$ before entering step 4. These four steps can be illustrated as Table 2.2:

$$\boxed{\begin{array}{c} \{\psi_a(kT_s)\}_{k=0}^{N-1} \rightarrow \{A_k\}_{k=0}^{N-1} \\ \Downarrow \\ \{L_\psi f(a, kT_s)\}_{k=0}^{N-1} \rightarrow \{B_k\}_{k=0}^{N-1} \\ \Downarrow \\ F_k = \sqrt{\frac{a}{2\pi}}\frac{B_k}{A_k} \\ \Downarrow \\ \{F_k\}_{k=0}^{N-1} \leftarrow \{f(kT_s)\}_{k=0}^{N-1} \end{array}}$$

Table 2.2: Flow of the reconstrction for $f(t)$.

2.6.3 Selection of Wavelet Functions

Among those commonly used wavelet functions, Morlet wavelet is the earliest wavelet function applied in CWT. The mathematical definition of Morlet is given in equation (2.11) as $\psi_0(t) = \pi^{-\frac{1}{4}} e^{j\omega_0 t} e^{-\frac{t^2}{2}}$. It is a complex wavelet that contains the real part and the imaginary part, represented by a solid wave and a dashed wave respectively in Fig.2.9(a). The frequency domain representation of Morlet is a single symmetric Gaussian peak, as shown in Fig.2.9(b), which provides a better localization result in both time and frequency domain than the sharp peak of a sinusoid.

In the Morlet wavelet equation (2.11), there is an admissibility condition of $\omega_0 > 5$. This ω_0 corresponds to the number of waves in Morlet. As shown in Figs. 2.9(a) and 2.9(c), the wave numbers are 6 and 20, respectively.

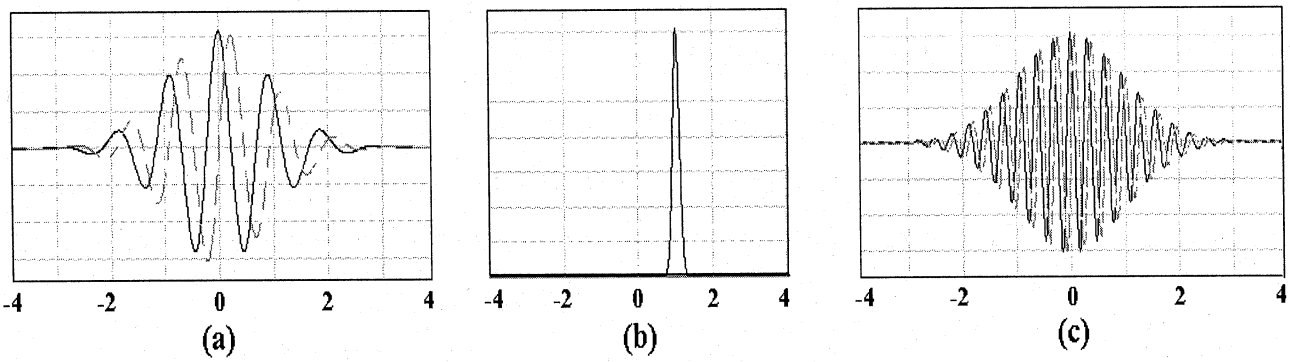

Figure 2.9: (a): Morlet wavelet with $\omega_0 = 6$. (b): Spectrum of Morlet wavelet in (a). (c): Morlet wavelet with $\omega_0 = 20$.

Another wavelet function usually used is the nth Gaussian derivative series of wavelet functions, which is also known as the Hermitian wavelets. The least number of this operator n is 2. This 2nd derivative of Gaussian is also known as a low-oscillation and complex-valued wavelet function named Mexican hat wavelet. Fig. 2.10 shows the Mexican hat and the 80th derivative of Gaussian, while the latter one actually is the Morlet function with a wave number of 12.

Fig. 2.11 illustrates a typical WRE signal decomposed by three wavelets: Morlet, Mexican hat and haar wavelets. Although the haar wavelet is a DWT wavelet basis, it is exhibited

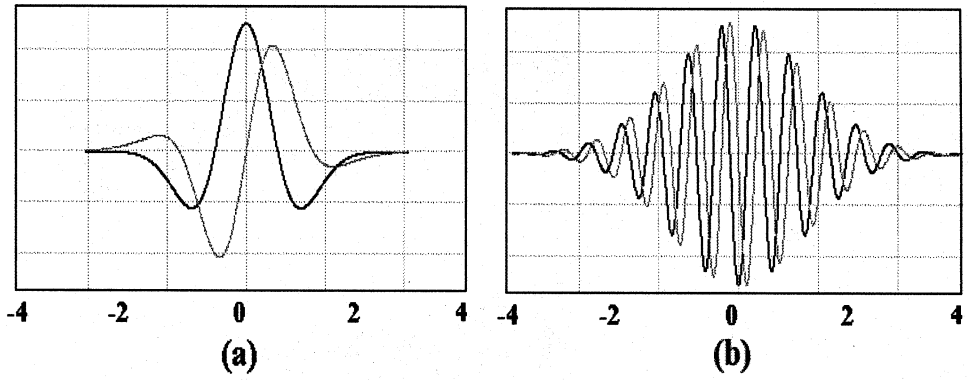

Figure 2.10: (a): 2nd derivative of Gaussian. (b): 80th derivative of Gaussian.

here to demonstrate the advantage of CWT in this research. It is clear that the haar wavelet decomposes the signal roughly especially on the abrupt changes, and it even results in a superfluous decomposition in the large scale part.

For the comparison of Morlet and Mexican hat, the displayed difference comes from the numbers of oscillation. Mexican hat wavelet blurred the signal more than Morlet wavelet, which is clearly shown as the amplitude variety and the abrupt changes on the edge of the signal. Therefore, the Morlet wavelet is selected for the WRE signal detection and auto classification work in this research, as it provides an excellent resolution on the joint time-scale plane.

2.6.4 Parameters Determination

In the implementation of CWT, three essential parameters must be defined: the start-scale, the end-scale and the incremental step of the scale. As CWT usually has an excellent resolution in large scale part but shrinks in small scale part, it is important to appropriately manipulate the scale parameters. Hence, for these three parameters, the start-scale operates the compression of small scale part, the end-scale controls the enhancement of large scale part, and the incremental step alters the total scale numbers and the granularity between two adjacent scales.

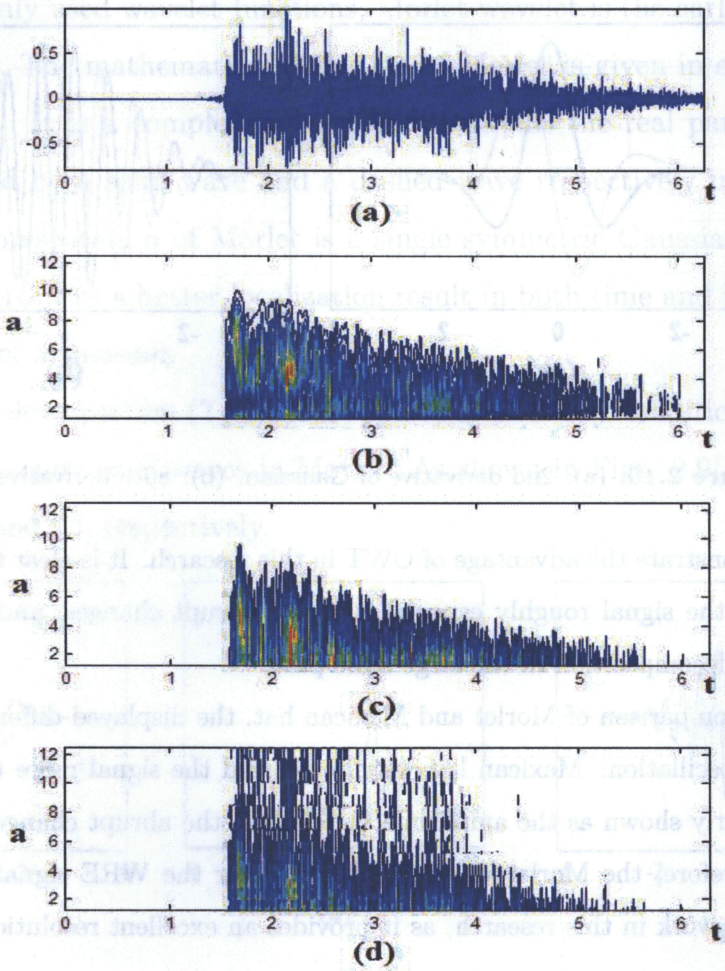

Figure 2.11: (a): Time domain of a typical WRE signal. (b): Morlet decomposition of the signal. (c): Mexican hat decomposition of the signal. (d)Haar decomposition of the signal.

Fig. 2.12 displays the difference of changing the start scale and the end scale separately. The left column is the value changing of the start-scale with constant values of the end-scale and the incremental step. It is apparently shown that the details in the small scale part alter with the changing of the start-scale parameter. The right column is only the value changing of the end-scale from which we can see that the large scale components are distinguished.

The incremental step is the most important parameter in the CWT computation. It

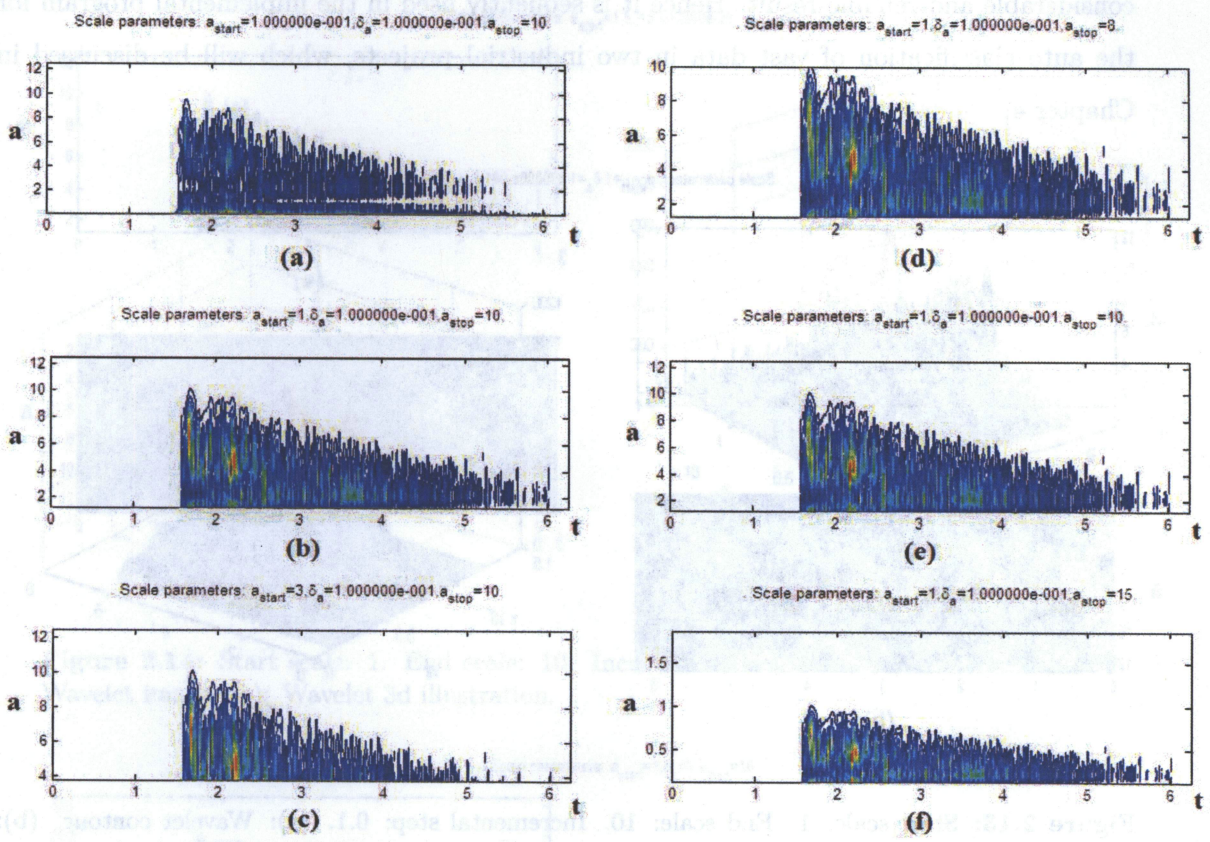

Figure 2.12: (a), (b) and (c): Constant values of the end scale and the incremental step with variational values of the start scale at 0.1, 1, and 3 respectively. (d), (e) and (f): Constant values of the start scale and the incremental step with variational values of the end scale at 8, 10 and 15 respectively.

handles how detailed the signal is projected into the time-scale plane. Therefore, if this parameter is too large, than the results will be cruder; if the parameter is too small, than the processing will be quite time consuming as too many details are calculated. Figs. 2.13, 2.14 and 2.15 makes the comparison of the above signal being processed with different incremental step values. From these figures it is clear that the resolution of wavelet decreases with the increase of incremental step proportionally.

Ultimately, these three parameters are set to be 1, 0.1, and 10, considering both resolution and time issues. Applied on the large amount of acoustic signals, this setting provides a

considerable and reliable result. Hence it is sequently used in the implemental program for the auto classification of vast data in two industrial projects, which will be discussed in Chapter 4.

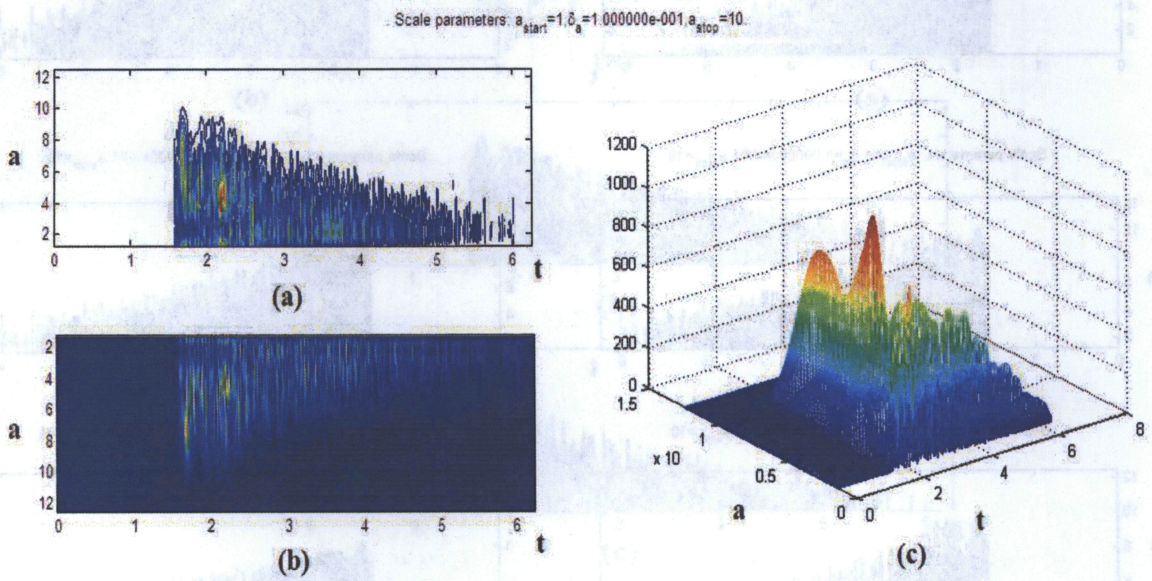

Figure 2.13: Start scale: 1. End scale: 10. Incremental step: 0.1. (a): Wavelet contour. (b): Wavelet image. (c): Wavelet 3d illustration.

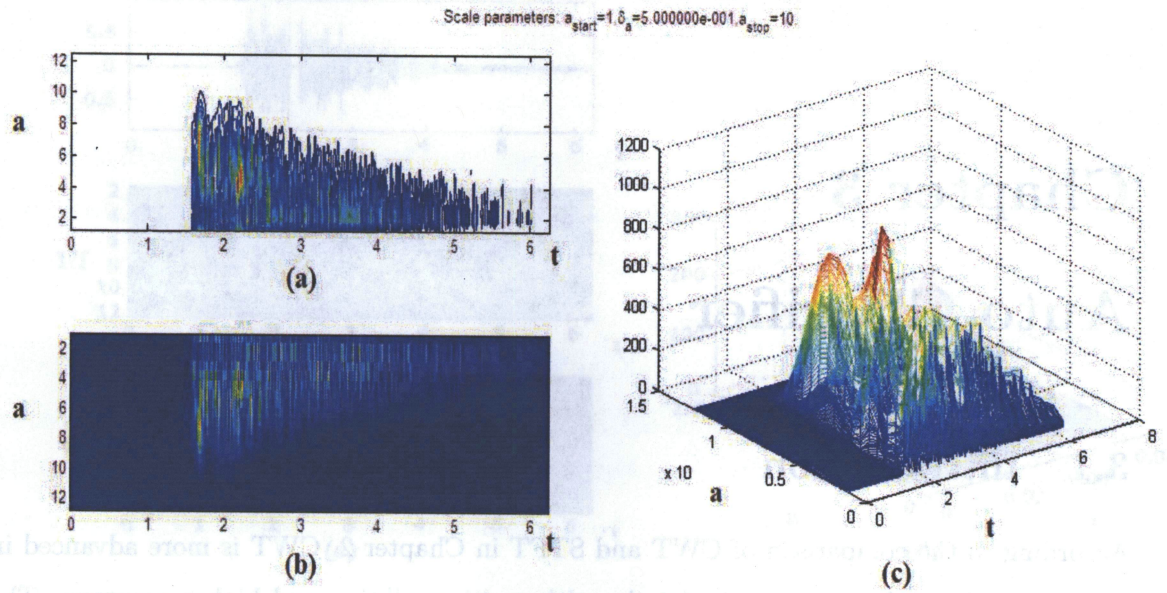

Figure 2.14: Start scale: 1. End scale: 10. Incremental step: 0.5. (a): Wavelet contour. (b): Wavelet image. (c): Wavelet 3d illustration.

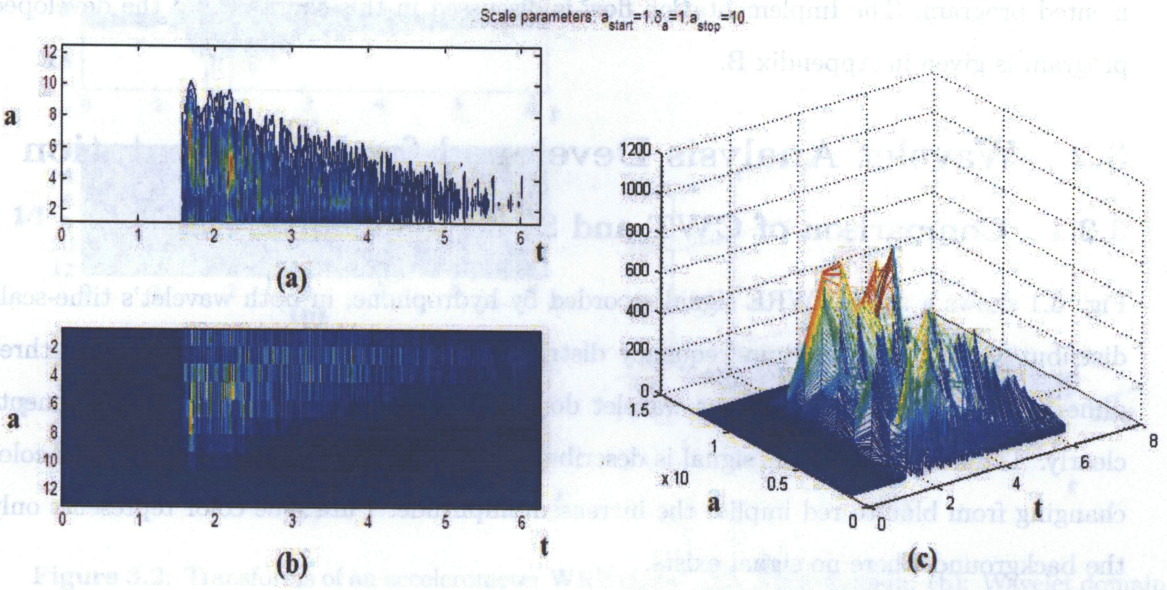

Figure 2.15: Start scale: 1. End scale: 10. Incremental step: 1. (a): Wavelet contour. (b): Wavelet image. (c): Wavelet 3d illustration.

Chapter 3

Auto Classifier

3.1 Introduction

According to the comparison of CWT and STFT in Chapter 2, CWT is more advanced in display joint time-frequency-scale details, with multi resolution and higher accuracy. The following section provides figured samples of typical WRE signals to show these advantages of CWT. Then they lead to the definition of the criteria for auto classifiers used in the implemented program. The Implementation flow is discussed in this chapter, and the developed program is given in Appendix B.

3.2 Wavelet Analysis Developed for Implementation

3.2.1 Comparison of CWT and STFT Techniques

Fig. 3.1 shows a typical WRE signal recorded by hydrophone, in both wavelet's time-scale distribution and STFT's time-frequency distribution, respectively. In addition, the three dimension (3D) illustration of the wavelet domain is given to show the scale components clearly. The amplitude of the signal is described in red and blue colors. Generally, the color changing from blue to red implies the increased amplitude. Pure blue color represents only the background where no signal exists.

Equation (2.10) shows the inverse proportional relationship of scale and frequency. As shown in Fig. 3.1(b), in wavelet domain, the signal starts at scale 10, which corresponds

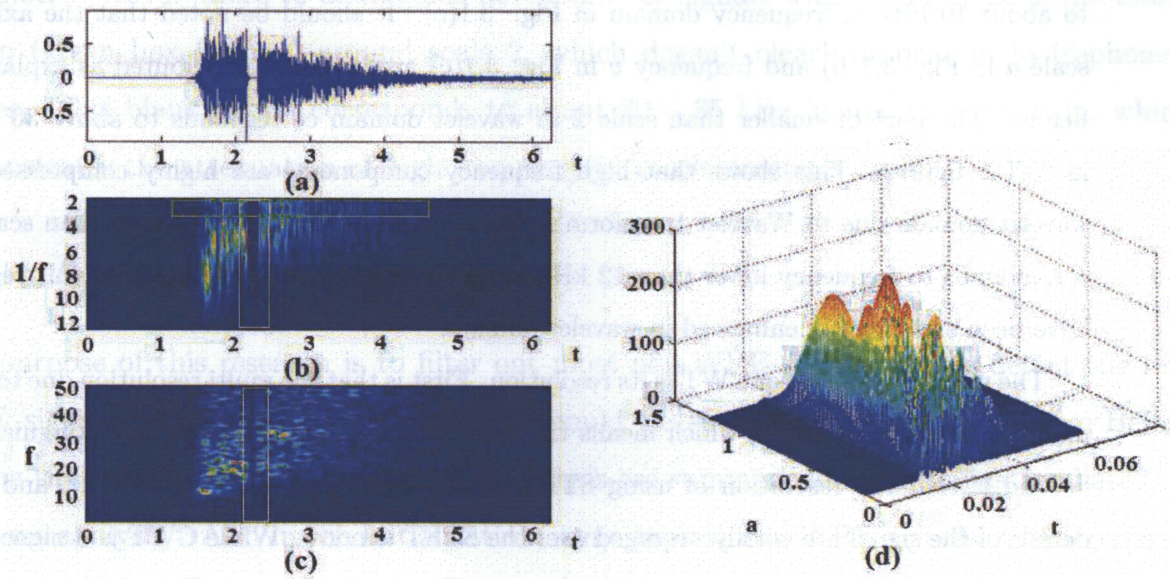

Figure 3.1: Transforms of a hydrophone WRE signal. (a): Time domain. (b): Wavelet domain. (c): STFT for the signal. (d): 3D illustration of the wavelet domain.

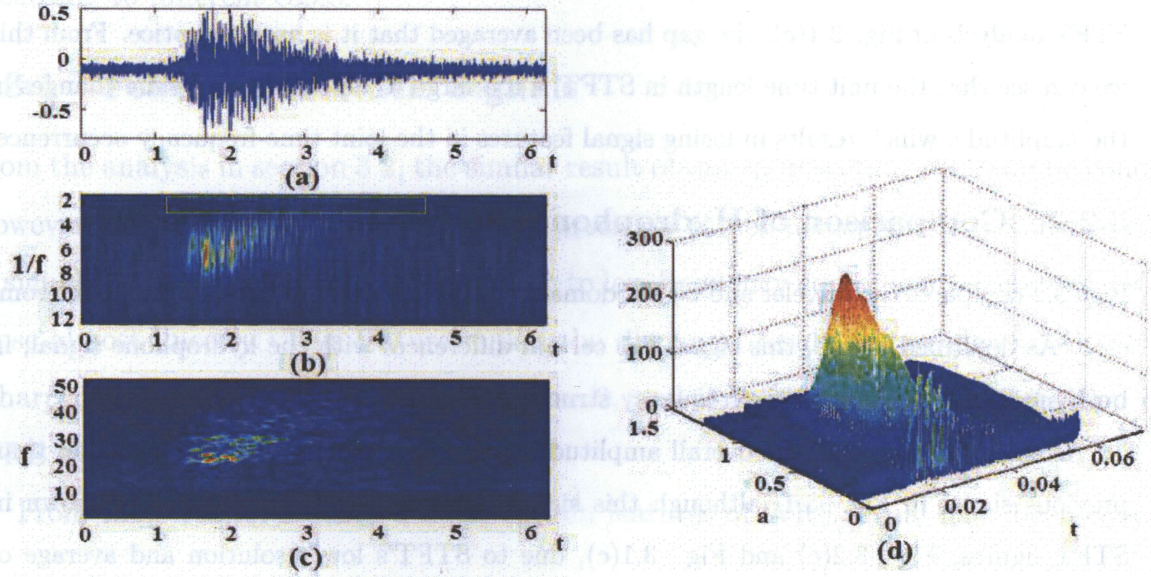

Figure 3.2: Transforms of an accelerometer WRE signal. (a): Time domain. (b): Wavelet domain. (c): STFT for the signal. (d): 3D illustration of the wavelet domain.

to about 10 kHz in frequency domain in Fig. 3.1(c). It should be noted that the axis of scale a in Fig. 3.1(b) and frequency v in Fig. 3.1(c) are inversely distributed as explained before. The part of smaller than scale 2 in wavelet domain corresponds to above 30 kHz in STFT figures. This shows that high frequency components are highly compressed in wavelet domain due to Wavelet transform's characteristics. The part of larger than scale 8 corresponds to frequency lower than 12 kHz in STFT figures, and the details in this region have been significantly enhanced in wavelet domain.

The main advantages of CWT is its resolution. First is that the multi resolution due to the inherent property of CWT, which means the resolution for different scales is distinguished. Second is that the resolution of using STFT in AE signal processing is too low, and the details of the signal are wholly averaged over the STFT window. While CWT is designed to exhibit the sharp discontinuities and fast changes. This is also shown in Figs. 3.1(a) and (b): in the time domain, there is a clear gap in the middle of the signal (white box framed), and in the wavelet domain this is apparently shown with the same gap length. However, in the STFT analysis of Fig. 3.1(c), the gap has been averaged that it is hard to notice. From this we can see that the unit time length in STFT is too large to detect the real-time changes of the amplitude, which results in losing signal features in the joint time-frequency occurrence.

3.2.2 Comparison of Hydrophones and Accelerometers

Fig. 3.2 compares the wavelet and STFT domain of a WRE signal recorded by an accelerometer. As described before, this signal has certain differences with the hydrophone signal, in both amplitude and joint time-frequency structure.

As shown in Fig. 3.2, the overall amplitude of this accelerometer signal is smaller than previous signal in Fig. 3.1, although this signal is normalized. This is clearly shown in STFT figures, Fig. 3.2(c) and Fig. 3.1(c), due to STFT's low resolution and average of those larger-amplitude details. Moreover, the 3D meshing models of wavelet in Fig. 3.2(d) and Fig. 3.1(d) also illustrate this phenomenon. For the hydrophone's 3D model in Fig. 3.1(d), there are several red hilltops in the signal duration. While for the accelerometer in

Fig. 3.2(d), there is only one clear peak.

Another feature here to distinguish accelerometer signals with hydrophone is the blank region (green box framed) around scale 2, which doesn't clearly appear in hydrophone's figures. This blank region corresponds to about $30 - 35$ kHz in frequency domain, which demonstrates the attenuation of high frequency in accelerometer's cases.

3.3 Auto Classifiers

The purpose of this research is to filter out most non-WRE signals and to detect the real WRE signals. Therefore, certain criteria should be set up as a dynamic filter. Before setting the criteria, features of ideal WRE signals are summarized for initialization based on previous analysis . Also in the initialization, some typical non-WRE signals' characteristics can be settled so as to enlarge the program's efficiency and accuracy. In addition, due to the different conditions of hydrophone and accelerometer, the features are distinguished according to different cases.

3.3.1 Features of WRE Signals

From the analysis in section 3.2, the similar result obtained in section 2.2.2 can be concluded. However, due to Wavelet transform's high precision and enhancement of the abrupt changes in signal,the large scale part, corresponding to low frequency component, decreases with time lapse almost linearly. This feature makes the displayed result quite different with STFT's "sharp of the knife" [1] as shown in Chapter 2, and it is essential for the detection of real WRE signals.

From the plentiful industrial data, certain features of WRE signal have been concluded:

- The energy should be concentrated in the main signal duration locating at 0.75s to 0.80s.

[1] This knife shape is also referred as "J" shape in the industrially.

- Less than 15% of the energy is distributed in the range of scale $a > 10$, corresponding to low frequency region of $f < 10kHz$.
- More than 25% of the energy is distributed in the range of scale $4 < a < 6$, corresponding to median and high frequency region of $15kHz < f < 25kHz$.
- More than 25% of the energy is distributed in the range of $2 < a < 4$, corresponding to median and high frequency region of $25kHz < f < 40kHz$.

These four features are measured under the condition that the energy of a real AE signal is concentrated in a narrow range of time band. In a word, most of the power should lie in the main duration of the signal. A large amount of noisy signals can be eliminated through pre-processing based on this feature. Wavelet analysis is not needed in this preprocessing. A power density ratio(PDR) is defined to measure the power inside a certain duration (0.75s to 0.80s) over the power of the whole signal. The three features related to scale factors are defined as large scale ratio(LSR), mid scale ratio(MSR) and small scale ratio(SSR), respectively.

Table 3.1: An example of thresholds for hydrophone and accelerometer WRE signals

	Hydrophone	Accelerometer
Power-density-ratio(PDR)	4.85%	4.25%
Large-scale-ratio(LSR)	15%	20%
Mid-scale-ratio(MSR)	25%	25%
Small-scale-ratio(SSR)	25%	15%

Table 3.1 gives an example of the parameters for above three features, where the project is conducted for waste water pipelines. The given ratios are calculated as following:

$$\begin{aligned}
\text{PDR} &= \frac{\text{the energy of signal from 0.75s to 0.80s}}{\text{the energy of the whole signal}} \\
\text{LSR} &= \frac{\text{the energy of signal in scale interval } a > 10}{\text{the energy of the whole signal}} \\
\text{MSR} &= \frac{\text{the energy of signal in scale interval } 4 < a < 6}{\text{the energy of the whole signal}} \\
\text{SSR} &= \frac{\text{the energy of signal in scale interval } 2 < a < 4}{\text{the energy of the whole signal}}
\end{aligned}$$

These parameters are designed to be tolerant enough not to miss weak WRE signals, but still get rid of most noise data. Based on the ratios of all the provided WRE signals, the thresholds are defined to be 20% wider than the lower bound and upper bound of these WRE ratios so as to allow possible weak signals pass the filter. With this tolerance to weak signals, the workability of filtering is still proven to be robust in Chapter 4.

In addition, as discussed in Section 2.2.2 and 3.2, hydrophones have greater sensitivity than accelerometers. It should be noticed that these features are distinguished for hydrophone and accelerometer, due to their different signal characteristics: the parameters chosen for hydrophone are more strict than accelerometer in all three features, as hydrophone signals have higher SNR and are easier to be detected.

3.3.2 Features of Typical non-WRE Signals

In the pipeline inspection, there always exist some typical non-WRE signals. Some of them are the ping signals made by technicians to test if the system works; some are vehicle related sounds generated by a car passing the cover of the pipe; and some are electric pops which have a very short duration. In addition, those mass and random noise composes the majority of non-WRE signals.

Set up criteria for these non-WRE signals not only helps to learn the physical features of acoustic signals' propagation in pipeline, but also greatly enlarges the efficiency and accuracy of the applied wavelet techniques. As wavelet requires multi-times convolution, it is computationally intensive, especially when used for large quantity of data. Therefore, if there is a pre-processing part to get rid of the obvious non-WRE signals, the wavelet processing procedure will be more efficient. Moreover, as mentioned in section 3.3.1 that those WRE features are quite tolerant which might result in greater false alarm probabilities, it will largely increase the accuracy of filtering out pre-defined non-WRE signals which might be mis-cataloged as WRE signals.

The main idea is to reduce the number of tested signals that require classification using wavelet techniques. In pre-processing part, only the PDR threshold are applied to distinguish

typical non-WRE signals and possible WRE signals. Some non-WRE signals will be classified with the wavelet features in the main processing procedure according to concrete demands.

Chapter 4 illustrates several types of non-WRE signals in two specific projects, and the observed features of these signals can be summarized as:

- Ping signals:

These signals can easily be filtered out by PDR thresholds. In the time domain illustration, these signals are quite concentrate and periodical inside its duration. The PDR of this type of signals are always larger than 0.99. While other types of signals including very large WRE signals never reach this high PDR based on our observation of large amount of data. Hence, it is stable and reliable to omit these ping signals with the threshold of 0.99.

- Electric pop signals:

Although the resource of generation is not clearly figured, these signals have the feature of very short duration with medium amplitudes. Their duration is usually less than $100ms$, which accounts about 1/5 of the main part that is processed. For these signals' filtering, the main processing part should be segment into 5 parts, and then the difference of PDR for each part is calculated. If the difference of part 1 with other parts are larger than a certain threshold, then the signal will be judged as electric signals.

- Miscellaneous signals:

As discussed in section 3.3.1, the power should be condensed inside signal's duration. While for miscellaneous signals, it is another case that the power is very scattered and locates randomly on the time-scale plane. The recorded data is most likely to be random noise if the PDR is too small, indicating that the energy is not concentrated around the certain spectrum. Thus, the threshold of PDR should be set up for filtering those less concentrated signals.

- Vehicle related signals:

Above three non-WRE signals are judged in pre-processing procedure. This type of signals is similar to WRE signals in the power distribution. However, there are more low frequency components in these signals than WRE signals. Basically, this kind of signal is emphasized not only for its characteristics, but to provide a customized non-WRE framework for further applications.

These signals are distributed mostly in low frequency ranges which means their LSR criteria will not be satisfied. However, they might pass the threshold of MSR and SSR. This would be a problem as the program is defined to classify a signal into WRE group if it satisfies at least two wavelet features. This can be solved by set up non-WRE criteria with LSR, that is, if the LSR is greater than the threshold, which means too many low frequency components, then the signal will be cataloged as non-WRE.

This can be further customized for shorter or longer scale ranges. The advantages of wavelet being a band pass filter can now be utilized. As either WRE or non-WRE signals are varying from different projects, pre-features of those signals should be acquired by experienced analysts at the very beginning, and then these auto classifiers should be applied to greatly save time and energy.

3.4 Implementations

3.4.1 Implementation Flows

The experiment is carried out in two steps: first, get rid of the obvious non-WRE signals in order to save storage and reduce computational demand; secondly, detect the real WRE signals. The algorithms of both wavelet and STFT exhibited in section 3.2 are implemented in Matlab 7.1 platform. The wavelet detection procedure is a six-step program, shown as following:

1. Extract only the main part of the signal, which locates at 0.75 to 0.80 seconds in the recorded duration.

2. Calculate the power-density-ratio (PDR) of the extracted signal over the whole signal:

If the ratio is larger than the threshold – consider as suspected WRE for further process;

If the ratio is smaller than the threshold – obvious non-WRE, filter out.

3. Compare the rest suspected WRE signal with the PDR characteristics of predefined non-WRE :

   If the signal falls into the range of predefined non-WRE characteristics, then it will be extracted to the non-WRE folder.

   If the signal does not satisfy the non-WRE characteristics, then it will be left in the suspected WRE folder.

4. Wavelet transform of the suspected WRE.

5. Compare the rest suspected WRE signal with the wavelet characteristics of predefined non-WRE:

   If the signal falls into the range of predefined non-WRE characteristics, then it will be extracted to the non-WRE folder.

   If the signal does not satisfy the non-WRE characteristics, then it will be left in the suspected WRE folder.

6. Calculate the scale ratio of transformed WRE, and signals satisfying following features will be extracted to the WRE folder:

   the large scale ratio (LSR) should be less than the threshold;

   the middle scale ratio (MSR) should be greater than the threshold;

   the small scale ratio (SSR) should be greater than the threshold.

In these six steps, the first three steps aim to get rid of most obvious non-WRE data, and they achieve desirable results. The last three are not always satisfied due to the variety of WRE, and the wavelet features should be modified according to particular practical demands. As this is an industrial application, the probability of miss detection should be as small as

possible. It is a compromised situation to sacrifice the detection accuracy. Therefore, in the real implementation, for the sixth step of wavelet filtering, it should be cautiously considered that how many features need to be satisfied, so as to reduce the miss detection probability. Sometimes it is necessary to add more scale features according to project demands. In the second project analyzed in Chapter 4, more criteria are addressed due to its specific requirements.

3.4.2 Computational Complexity

As the method and algorithm will be fully implemented in embedded system for industrial installation, it should minimize the processing time. Otherwise there might be missed signals during the processing time.

In the fourth step, when doing wavelet transform, signals with more details and noise usually take longer to process. It is essential to get rid of the obvious non-WRE signals before wavelet transform procedure. Therefore, the first three steps of PDR filtering should be robust enough to filter out as many non-WRE signals as possible, while passing all the WRE signals.

Although the computation of PDR in the pre-processing is very easy, the threshold of PDR used in the first round of filtration has a large impact on the computational complexity of the second round of analysis that involves wavelet transform. A higher PDR threshold reduces the computational demand of the wavelet process but may result in missed detection of the weak WRE signals. Fewer WRE signals will be miss-detected but the processing becomes more complex if a lower PDR threshold is used. Different thresholds for hydrophone and accelerometer are used to produce the results presented in the following section. These thresholds are selected according to different practical requirement. The parameter selection work will be thoroughly discussed in Chapter 4 with the examples in industrial projects.

3.4.3 Introduction to the Program

This program is developed based on Matlab's GUI interface. It is designed to be compilable and executable also on computers without Matlab. Some of the program's functions are described in Appendix B, mainly focusing on the customization of those WRE and non WRE features.

Chapter 4

Resulted Analysis

4.1 Introduction

Two projects provided by a pipe inspection company [1] are analyzed in this chapter in-depth. HOW and EPWU are the abbreviated name for these two projects, respectively.

At the beginning of each project, the ideal procedure of integrating our research with the company's AET technology is developed as:

1. In the pre test stage:
   samples of WRE signals and typical non-WRE signals must be provided to determine the classification criteria such as how many thresholds should be used, what ratio should be set for each threshold, how to treat the interaction of these thresholds, and how to determine the relationship between the thresholds and the classification work, etc;

2. In the main test stage:
   the daily coming data should be processed by both wavelet analysis and their previous STFT software in parallel, and both processing procedure should not be affected by each other;

3. In the post test stage: the result of both processing method will be compared regarding the accuracy and efficiency issue.

[1] The Pressure Pipe Inspection Company Ltd. Website:www.ppic.com

The accuracy is described as reducing the probability of miss alarm (MA) and false alarm (FA) as much as possible. Here MA represents a real WRE signal that is not detected; and FA represents a noise signal that is falsely detected as WRE signal. Between MA and FA, MA is regarded as much more critical than FA in this research. This is because a MA will not be discovered in the following processing procedure, as a real WRE signal is quite rare in the large amount of raw data. However, although FA can be detected by an analyst in a second round classification, it still need to be reduced to save energy.

The efficiency is depicted as the time consuming, the computer complexity and the labor cost issues. Compared with the company's previous analyzing procedure, the wavelet auto classification that we've developed greatly save the cost of operation. While with the previous technique, they need at least 2 analysts to work for a whole project. In addition, as processing the data and discriminating signals using eyes and ears are such tedious and biased works, they need different people to double check the results in case some weak signals have been omitted. While with the help of the auto classifier, most of the raw data processing can be done automatically with a reliable result. Therefore, the analysts just need to further confirm the result, which will account only 10% to 20% of their previous work.

Our research targeted for these two projects is to apply wavelet analysis in the acoustic signal processing, and build up auto classifier groups to detect the WRE signals. The classifier will classify the raw data into the three categories (non-WRE, sus-WRE and WRE) automatically, meanwhile greatly save the energy for labor works.

4.2 Analysis for the First Project (HOW)

4.2.1 Project Background

This project is conducted based on the contract of a county government in US collaborating with the company. The main target of the project is to evaluate the condition of a PCCP (shown as Fig. 2.1) with the company's patent AET technology. The tested portion was found to be deteriorating in a previous monitoring. After being alerted to the deterioration, the government hired technicians to do a corrosion survey and was informed that the cor-

rosion came from some stray currents. Thus, the government cooperated with the company to further monitor this previously deteriorating portion of the pipeline.

The whole pipeline portion that was inspected covers an overall distance of 1,543 meters located in Columbia, Maryland as shown in Fig. 4.1. The pipeline was still in service when monitored. After the inspection, the company concluded the test result and gave a report about the localized deterioration of the inspected portion. Then this portion will be subjected to further analysis and even repair based on the conclusion of the report.

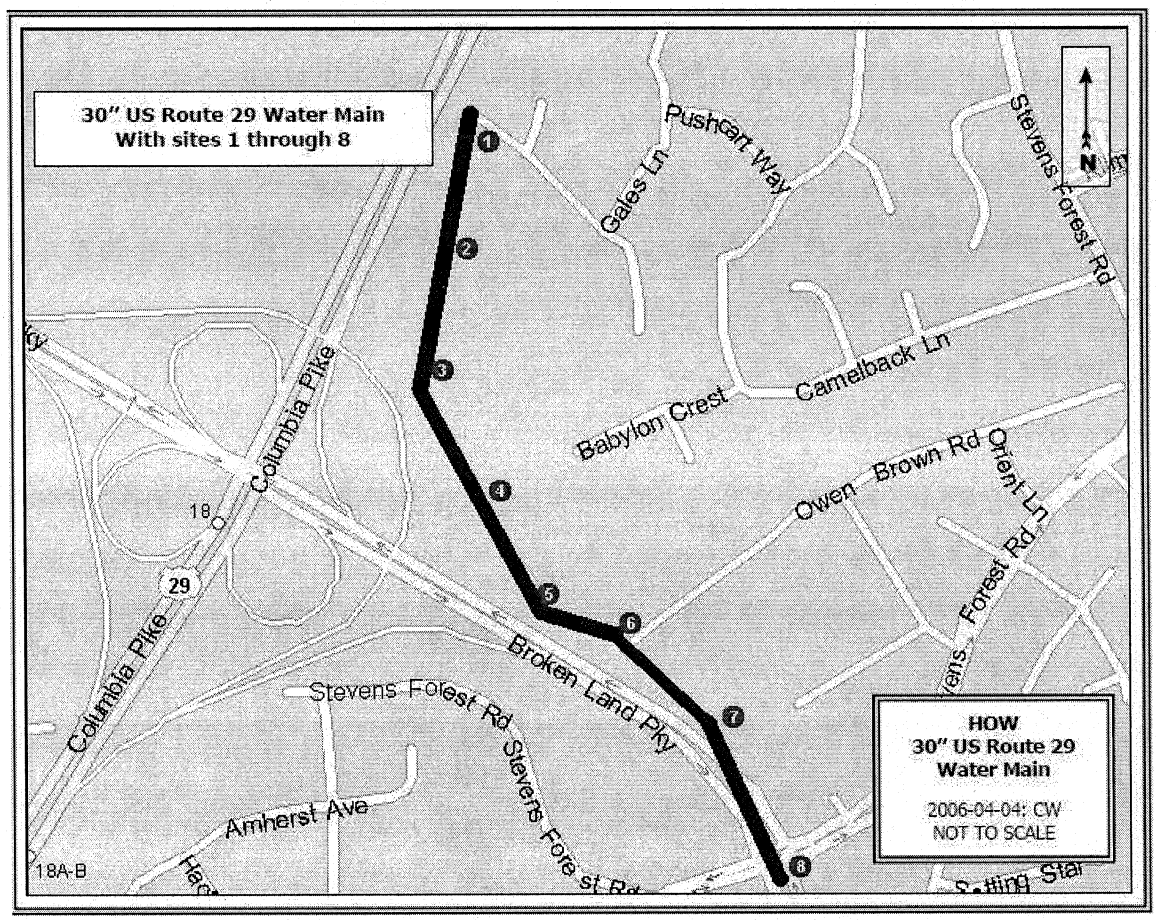

Figure 4.1: Map of the sites.

Having the purpose of validating its AET technology and confirming the pipeline's deterioration, the company started the installation of the equipment in January 2006, and monitored from February 2006 to August 2006. During their 2880 hour monitoring period,

the analysts of the company used their previous STFT software to process the data, and then classified the data manually into categories of WRE, suspected WRE and non-WRE. In the category of WRE, those confirmed signals require a GPS localization process and are further cataloged into the localized WRE signal group or the unlocalized signal group. Those localized signals will be reported to help evaluate the condition of the pipeline. The rest unlocalized signals will be considered as a backup for the decision of the criteria and a source for checking sensors.

As this project was finished before our research, the wavelet analysis is based on large quantity of raw data in this project, and the company's previous conclusion is taken as the benchmark of the research. As discussed in Chapter 3, the criteria of classifying hydrophone signals and accelerometer signals are different, the sensor information and site spacing are given in Table 4.1. The numbers in 'distance' row are given as the distance (in feet) between the corresponding site and the previous site. In the 'sensor' row, HYD represent hydrophones and ACC represent accelerometers.

Table 4.1: Site and sensor information for project 1.

Site	1	2	3	4	5	6	7	8
Distance	NA	386	607	536	690	370	670	673
Sensor	HYD	ACC	ACC	HYD	HYD	HYD	ACC	ACC

4.2.2 Wavelet Analysis and Criteria of Features

Wavelet Analysis

Fig. 4.2 and Fig. 4.3 provide four sample WRE signals recorded by hydrophones and accelerometers respectively, which are part of the sample WRE signals used as benchmarks of the feature extraction procedure. Fig. 4.4 shows three types of non-WRE signals, and they are also embedded in the program for automatical batch processing in this project. Each subfigure in these figures are named in a form of an alphabet with a number. Different alphabet represents different signal and the specific number represents the illustration method. For example, $(a1)$ means this is the first signal in the figure using a 2-dimension illustration

technique, and ($b2$) donates the second signal in the figure with a 3-dimension illustration.

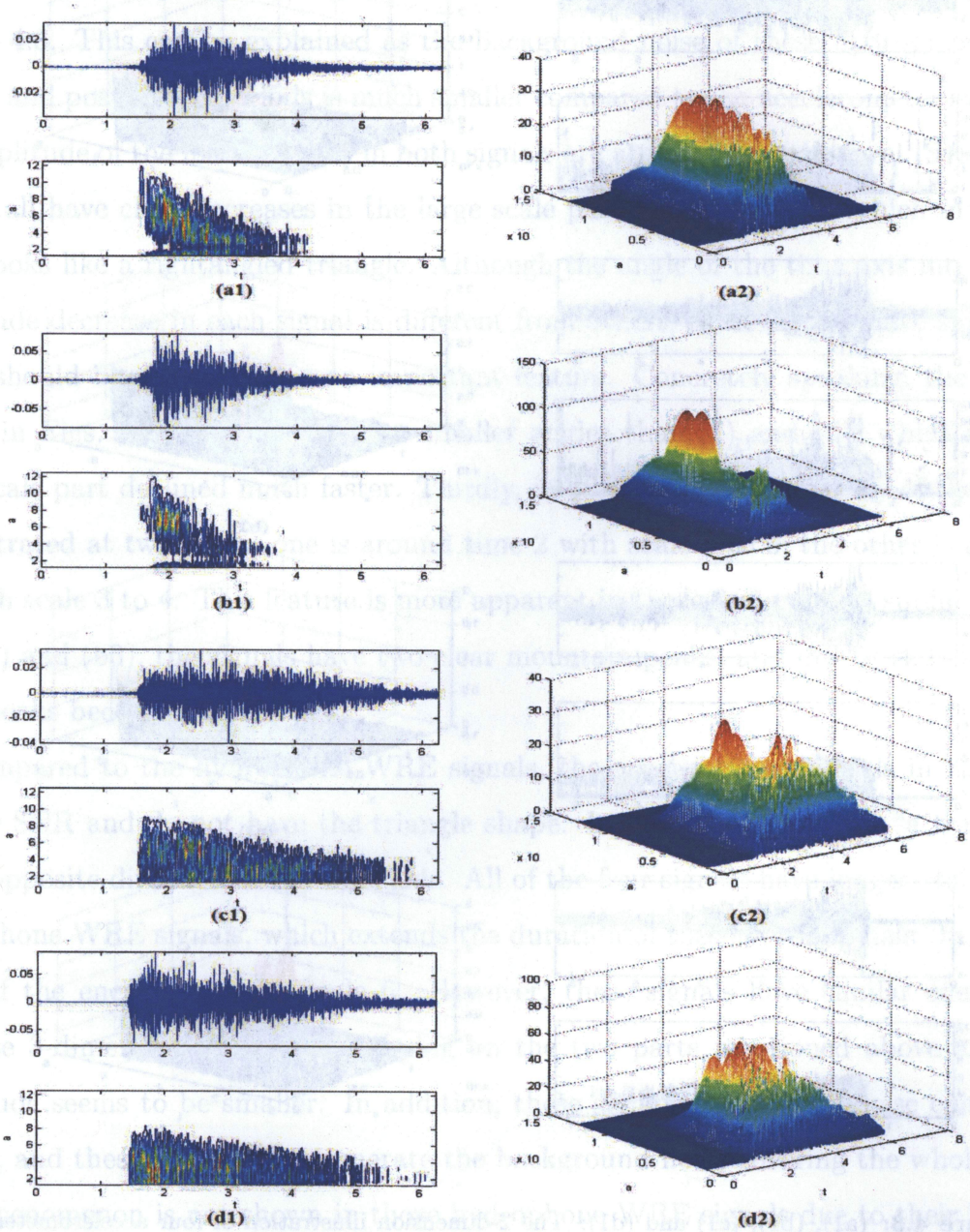

Figure 4.2: (a1), (b1), (c1) and (d1): The 2-dimension illustration of four hydrophone WRE signals. Top subfigures show time domain and bottom subfigures display wavelet domain. (a2), (b2), (c2) and (d2): The 3-dimension illustration of these signals.

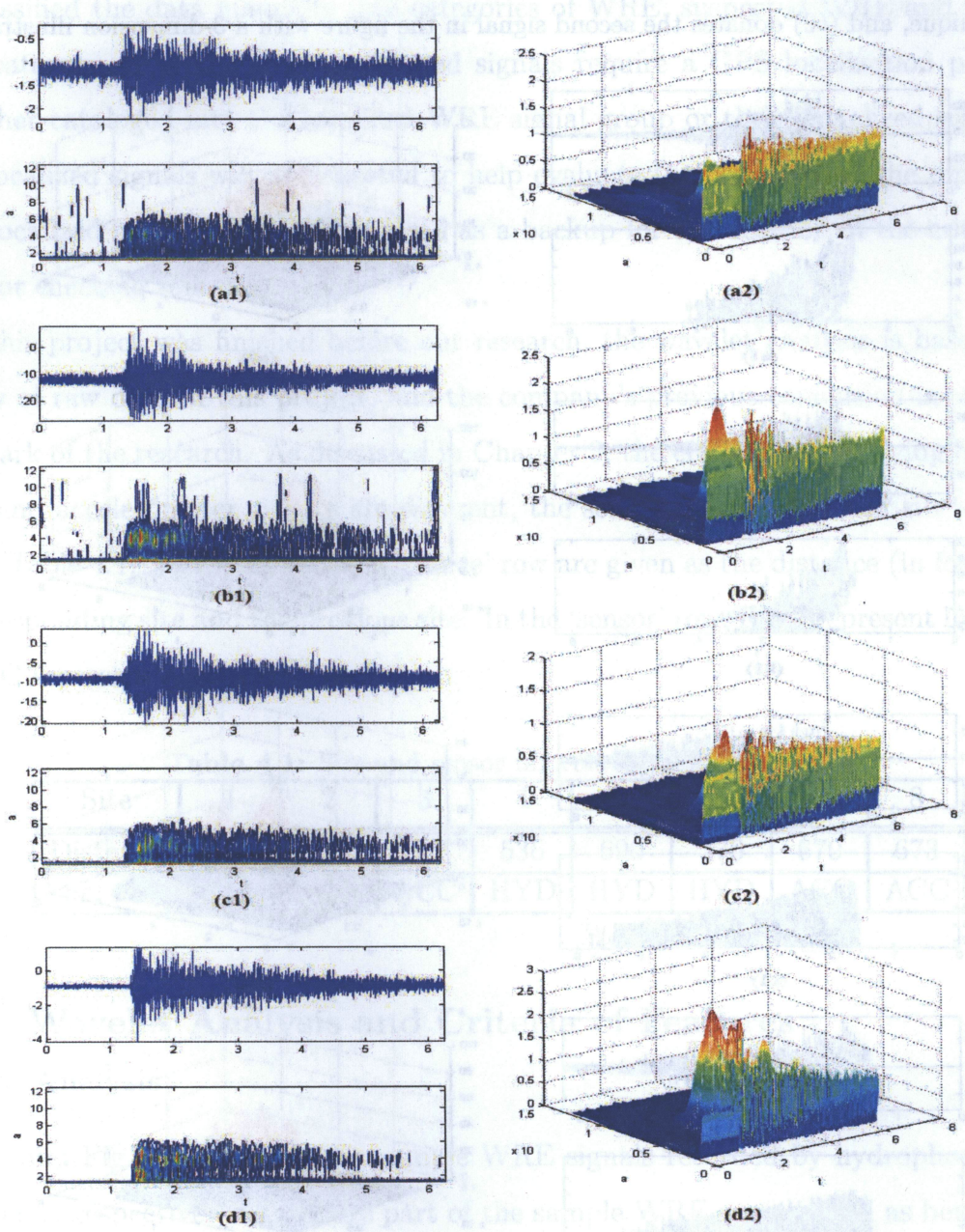

Figure 4.3: (a1), (b1), (c1) and (d1): The 2-dimension illustration of four accelerometer WRE signals. Top subfigures show time domain and bottom subfigures display wavelet domain. (a2), (b2), (c2) and (d2): The 3-dimension illustration of these signals.

The four hydrophone WRE signals shown in Fig. 4.2 have certain common characteristics. First, although all the tested signals are normalized to the same scale of energy, apparently the SNR of these hydrophone signals are much larger than the accelerometer signals shown in Fig. 4.3. This can be explained as the background noise of these hydrophone signals in the pre and post signal periods is much smaller compared to the accelerometer signals, while the amplitude of the main portion in both signals are at the same scale level. Secondly, these signals all have clear decreases in the large scale part almost linearly, which makes each of them looks like a rightangled triangle. Although the angle of the time axis intersecting the amplitude decrease in each signal is different from others, these signals have similar shapes which should be considered as an important feature. Concretely speaking, the two signals shown in Figs. 4.2 (a) and (b) have smaller angles than (c) and (d), which means their large scale part declined much faster. Thirdly, in each signal the majority of the energy are concentrated at two parts: one is around time 2 with scale 5 to 6; the other is around time 2.5 with scale 3 to 4. This feature is more apparent in those 3-dimension subfigures. In Fig. 4.2 (b2) and (b3), the signals have two clear mountain peaks; and in Fig. 4.2 (b1) and (b4) these peaks becomes clusters.

Compared to the hydrophone WRE signals, the accelerometer signals in Fig. 4.3 have smaller SNR and do not have the triangle shape. In fact, they look like "a train" running on an opposite direction of the time axis. All of the four signals have longer "tails" than the hydrophone WRE signals, which extends the duration of these WRE signals. In each signal, most of the energy is under scale 6. However, these signals have similar energy clusters in those 3-dimension subfigures focusing on the two parts mentioned above although the amplitude seems to be smaller. In addition, these signals have larger noise components at scale 1, and these components generate the background noise covering the whole time axis. This phenomenon is not shown in those hydrophone WRE signals due to their larger SNR. While for the accelerometer WRE signals after normalization, both the signal part and the noise part have been enlarged, hence this noise become visual. This kind of noise can be removed using wavelet reconstruction method.

All in all, it is further demonstrated that different thresholds should be set for the hydrophone WRE signals and the acceleromter WRE signals. Because of the difference between these two types of signals such as duration, energy location and the time-scale shape, they should be discriminated.

Fig. 4.4 provides three typical non-WRE types in this project. All of them can be filtered out with PDR filtering discussed in Chapter 3. In the subfigures, Fig. 4.4 (a) is a periodical background noise, (b) is a beep signal produced by technicians to test the connecxity of the sensors, and (c) is a miscellaneous noise signal with certain scale bands(the illustrated signal has a centralization around scale 1.5 to 2.5).

The first and third signal can be filtered out because their energy does not dominantly fall into the range of the main signal duration. However, sometimes the third type of signal may pass the PDR threshold, and it still can be further processed with a customized non-WRE type aiming at getting rid of particular scale-bands signals. The second beep signal concentrates on the main signal part, but the PDR is too high (> 0.99), while the real WRE signals never reach this high PDR according to previous experience and our test results. Hence this type can be easily excluded by setting the upper bound of PDR.

Criteria of Features

Table 4.2: Thresholds of hydrophone and accelerometer WRE signals for project 1.

	Hydrophone	Accelerometer
Power-density-ratio(PDR)	4.85%	4.35%
Large-scale-ratio(LSR)	15%	15%
Mid-scale-ratio(MSR)	25%	30%
Small-scale-ratio(SSR)	25%	20%

Table 4.2 lists the thresholds for hydrophone WRE and accelerometer WRE respectively. Generally speaking, the criteria for hydrophone is more stringent than for accelerometer. However, as shown in the last section, the accelerometer WRE signals have more mid-scale components at scale 4 to 6 and less large-scale components above scale 8, the criteria has been modified.

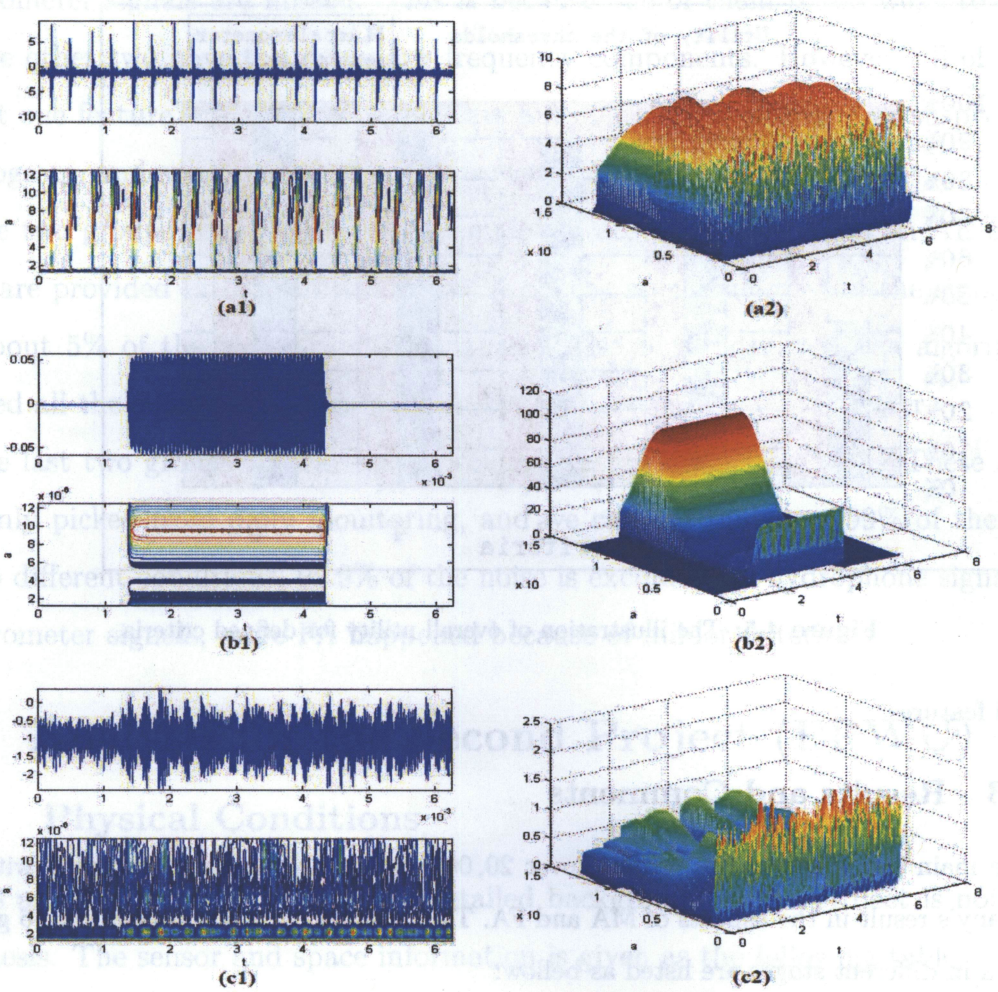

Figure 4.4: (a1), (b1) and (c1): The 2-dimension illustration of three typical noise's types. Top subfigures show time domain and bottom subfigures display wavelet domain. (a2), (b2) and (c2): The 3-dimension illustration of the noise.

In the pre test stage of this project, we've selected over 2000 samples from the whole data space to evaluate the workability of these criteria. If these three thresholds are used separately, the order of filtering ability is: LSR > SSR > MSR.

The illustration of overall utility for hydrophone and accelerometer is shown in Fig. 4.5, where the five pairs of bars represent the use of: 1) PDR; 2) PDR and LSR; 3) PDR, LSR and SSR; 4) PDR, LSR, SSR and MSR; 5) PDR, LSR, SSR, MSR and customized non-WRE

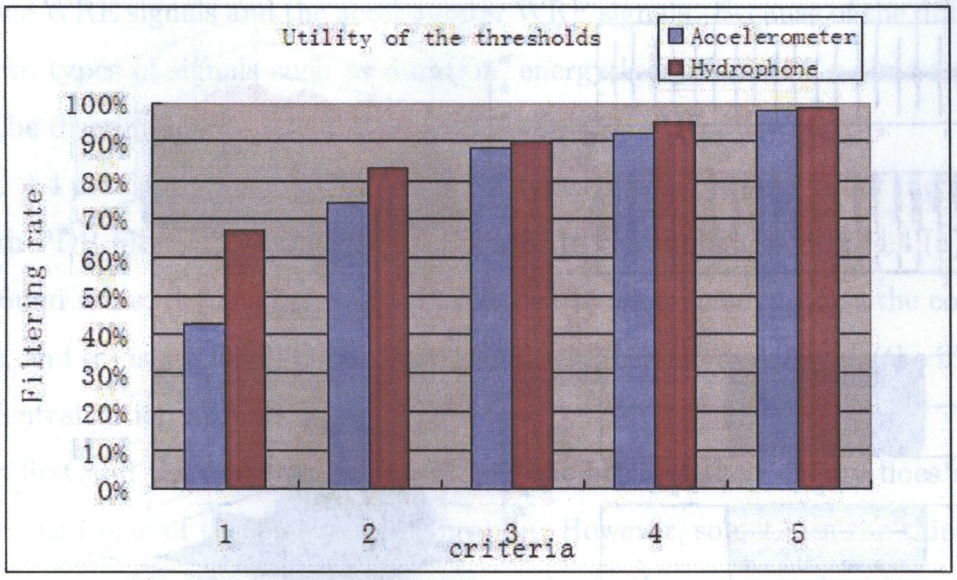

Figure 4.5: The illustration of overall utility for defined criteria.

signal features.

4.2.3 Results and Comments

In the main test stage of the project, over 20,000 signals are tested to compare with the company's result in the aspects of MA and FA. To provide a detailed observation , 6 groups of data in different stages are listed as bellow:

Table 4.3: Results of 6 tested groups.

	1	2	3	4	5	6
Type	ACC	HYD	ACC	HYD	ACC	HYD
Tested	41	28	89	269	517	756
Detected	38	28	11	15	66	2
Confirmed	41	28	3	14	3	0
MA	3	0	0	0	0	0
FA	0	0	8	1	63	2

In Table 4.3, the first two groups are all confirmed WRE signals for accelerometer (ACC) and hydrophone (HYD), respectively. These WRE signals were collected in the previous

test of the same pipeline. It is shown that hydrophone signals are all detected, while three accelerometer signals are missed. This is because one of them is too weak to be detected, and the other two have too many low frequency components. However, all of them satisfy at least one feature. Thus, these signals are automatically considered as suspected-WRE in the program, and subjected to further inspection.

The two groups in the middle are samples of observed data when an AE event occurs, which are provided in the pre test stage. It can be seen that most of the signals are noise, and about 5% of the data are WRE signals. Also it is clear that the algorithm claimed detected all the signals, and especially in hydrophone case it works better.

The last two groups are raw data provided in the main test stage. These are the data randomly picked from daily monitoring, and we can see that over 99% of them are noise. Due to different conditions, 99.9% of the noise is excluded for hydrophone signals; while for accelerometer signals, more FA happened because of milder criteria.

4.3 Analysis for the Second Project (EPWU)

4.3.1 Physical Conditions

This is an ongoing project, thus the detailed background of the project is not provided in this thesis. The sensor and space information is given as the following table:

Table 4.4: Site and sensor information for project 2.

Site	1	2	3	4	5	6	7
Distance	NA	500	490	521	515	546	554
Sensor	ACC	HYD	ACC	ACC	ACC	HYD	ACC
Site	8	9	10	11	12	13	14
Distance	507	465	529	911	475	528	474
Sensor	ACC	ACC	HYD	HYD	ACC	ACC	ACC

4.3.2 Wavelet Analysis

As this is a project started from February 2008, not many WRE signals are collected, and we are in the pre test stage. However, the feature of WRE signals in this project is slightly different from those in the first project. Fig. 4.7 shows a confirmed WRE signal recorded by four sensors. In these four sensors, the two at site 6 and site 10 are hydrophones, and the other two at site 8 and site 9 are accelerometers. Fig. 4.6 shows the location of these sensors where black squares represent the signal being recorded by the sensor, and white squares means the signal is not picked up. Hydrophones are squares pass through the pipeline, and accelerometers are squares on the pipeline. The symbol of 's' with a number donate the sensor's site, such as 's7' represent site 7.

The AE event occurred between site 8 and 9, and it was closer to site 8 as shown in Fig. 4.6. Hence, after passing two sensors, the signal is picked up by site 6 and 10, as these two sensors are hydrophones. Sensor 7 did not detect the signal because it is an accelerometer which is not sensitive enough at that distance.

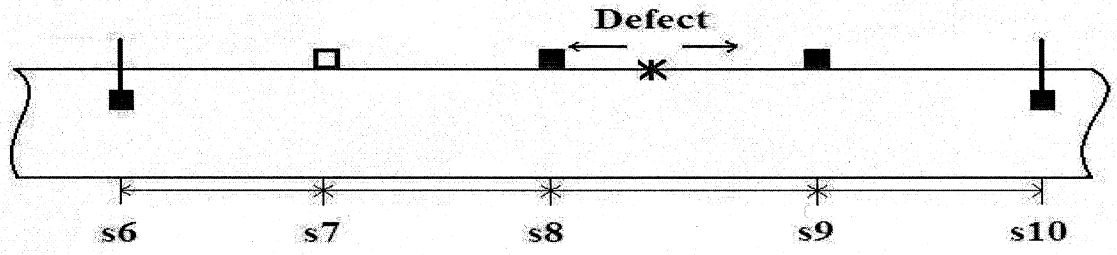

Figure 4.6: Diagram of the site information.

In the subfigures of Fig. 4.7, (a), (b), (c) and (d) show the signal recorded by site 8, 9, 10 and 6 respectively. (a) has the largest amplitude, and has two main scale bands centralized at scale 6 and 3. While after propagating, the signal attenuates in (b) and (c). However, the amplitude of (c) is larger than (b) although site 10 is farther than site 9. This difference attests to the greater sensitivity of hydrophones. Besides, the two scale bands have changed in (b), (c) and (d): the energy cluster at scale 3 disappears, which demonstrates

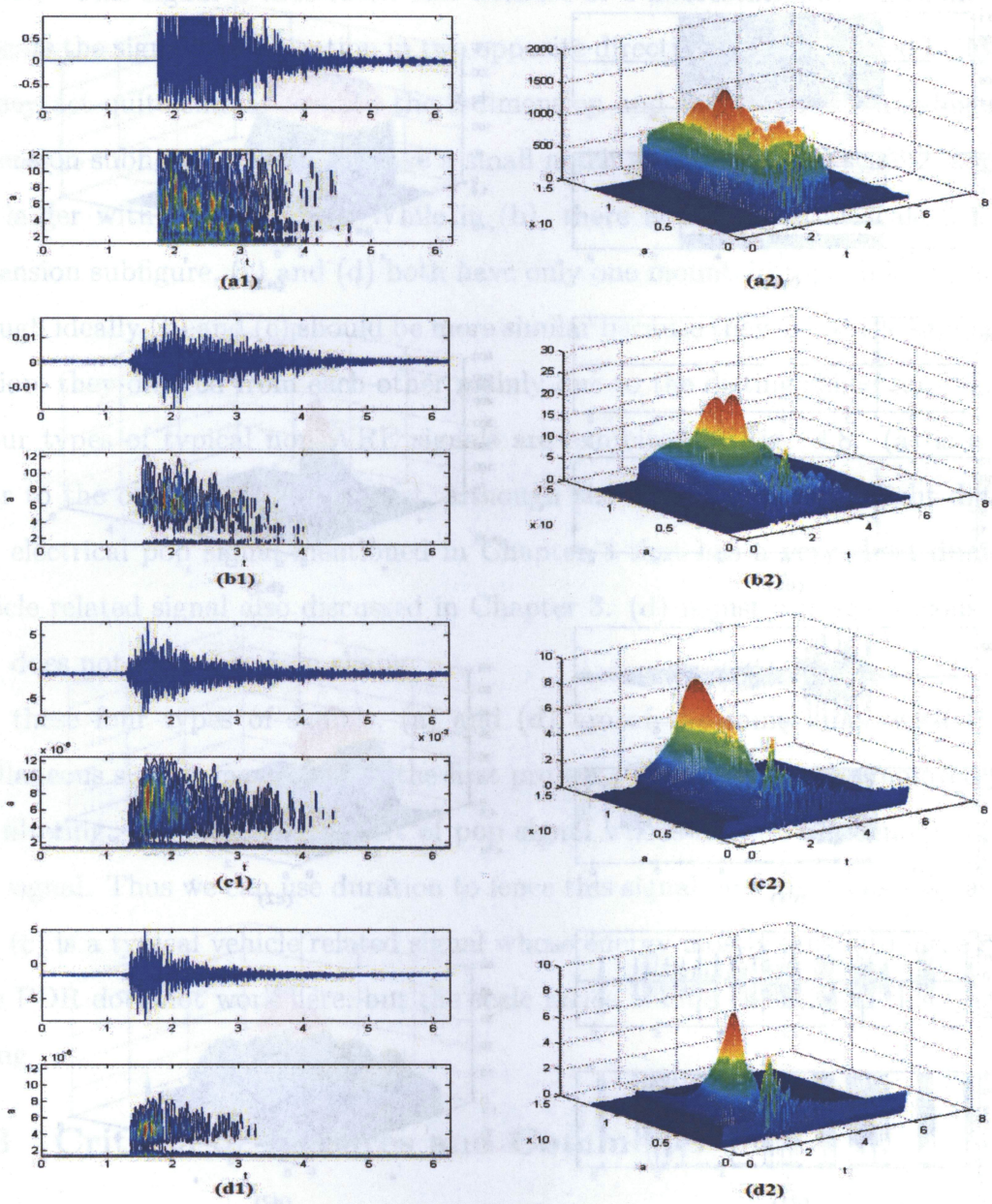

Figure 4.7: (a1), (b1), (c1) and (d1): The 2-dimension illustration of the WRE signals for site 8, 9, 10 and 6, respectively. Top subfigures show time domain and bottom subfigures display wavelet domain. (a2), (b2), (c2) and (d2): The 3-dimension illustration of these signals.

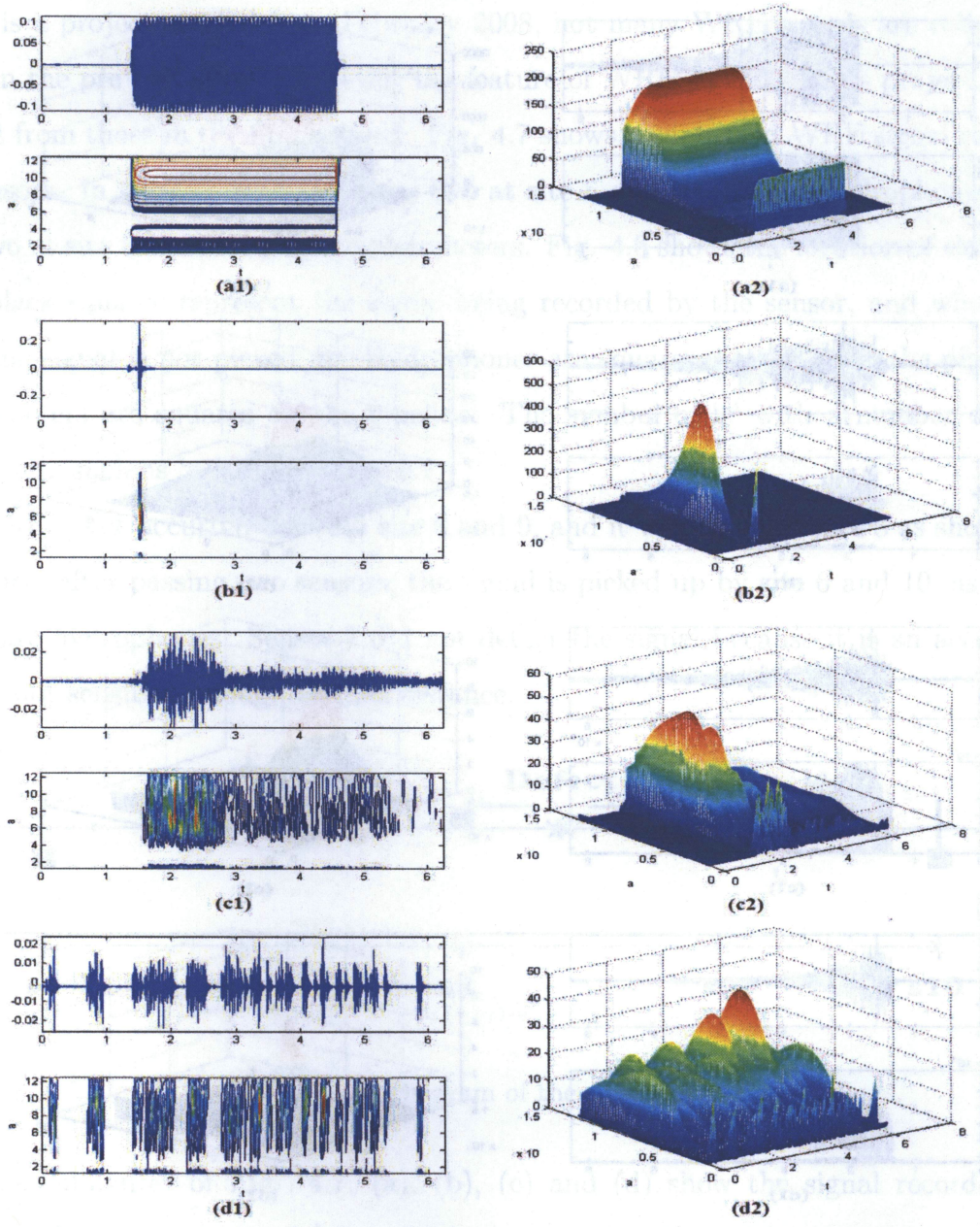

Figure 4.8: (a1), (b1), (c1) and (d1): The 2-dimension illustration of four typical noise's types. Top subfigures show time domain and bottom subfigures display wavelet domain. (a2), (b2), (c2) and (d2): The 3-dimension illustration of the noise..

the attenuation of the high frequency in this project is much faster than that of the middle frequency. This signal is illustrated also because of a interesting phenomenon. (c) and (d) represents the signal's propagation in two opposite directions both recorded by hydrophones, and they act quite similar in both the 2-dimension and the 3-dimension subfigures. In the 2-dimension subfigure, they both have a small notch at time 1.5 and scale 2, and this notch splits larger with time lapsing. While in (b), there is a big gap at scale 2 to 4. In the 3-dimension subfigure, (c) and (d) both have only one mountain top while (b) has two tops. Although ideally (b) and (c) should be more similar because they are at the same propagation direction, they differed from each other mainly due to the distinguished sensors.

Four types of typical non-WRE signals are exhibited in Fig. 4.8. (a) is a ping signal similar to the one in the first project, although the scale bands have slight difference. (b) is the electrical pop signal mentioned in Chapter 3 that has a very short duration. (c) is a vehicle related signal also discussed in Chapter 3. (d) is just a miscellaneous noise signal which does not have a certain shape.

In these four types of signals, (a) and (d) are of the same kinds with the ping and miscellaneous signals mentioned in the first project. Thus they can be removed easily using PDR filtering. (b) represents a sort of pop signal whose duration is usually 1/10 of a real WRE signal. Thus we can use duration to fence this signal, and this is as easy as calculating PDR. (c) is a typical vehicle related signal whose energy mostly falls into large scale ranges. Hence PDR does not work here, but the scale ratios will be essential in this type of signal's filtering.

4.3.3 Criteria of Features and Comments

As this project is proceeding, the final confirmed result is not provided yet. However, based on the above information and the recommendation of technicians in the company, more criteria are settled. Two scale band ratios are added to restrict the WRE features as shown in Table 4.5. These two ratios have a relationship of 'OR' as shown in the program's diagram in Fig. B.3. Hence there will be 5 ratios together in the wavelet filtering procedure. The

computer will judge the signal to be WRE if it satisfies at least one feature of LSR, MSR, and PDR as well as one of the scale band ratios.

Other thresholds are also adjusted in this project. The amplitude of the signals in this project are larger than the first project, thus the PDR is greater. This may be various according to the pipeline and the water condition. Besides, the three wavelet ratios are not that stringent as they have some overlap with the scale band ratios. Before applying the two scale band ratios, the filtering ability was 63% without setting typical non-WRE features and 76% with setting those features. While with the criteria shown in Table 4.5, the program is able to get rid of 89% of raw data, which means its efficiency has been greatly raised.

Table 4.5: Thresholds of hydrophone and accelerometer WRE signals for project 2.

	Hydrophone	Accelerometer
Power-density-ratio(PDR)	5.25%	4.65%
Large-scale-ratio(LSR)	15%	15%
Mid-scale-ratio(MSR)	23%	25%
Small-scale-ratio(SSR)	25%	20%
scale-6-ratio	20%	15%
scale-3-ratio	10%	5%

Chapter 5

Conclusion and Future Works

5.1 Conclusion of the Thesis Work

This thesis demonstrates that wavelet transform is a robust decomposition technique for non-stationary signals. Also the time-scale analysis is a powerful tool in extracting detailed features, and detecting signals under inspection.

Compared with TF methods, time-scale analysis has the advantages of multi-resolution and better precision. Its ability better than several TF methods of digging into the details of signals had been further proved in this thesis. It is well known that a signal can be depicted as the sum of infinite or finite sine and cosine functions. This sum is the Fourier expansion. However, the major disadvantage of Fourier expansion and Fourier transform is that it has only the frequency resolution and no time resolution. Like statistic parameters only reveal the averaged information of a signal in time domain, the spectrum displays all the frequency components in a signal. Nevertheless, the time information, such as when exactly they present cannot be provided. Therefore TF methods are developed to cut the signal into small parts, and display the spectrum for each part separately. Finally the sum of spectrum in each part is collected and distributed over the time domain to give the whole time-frequency joint representations. However the size of the cutting work in TF methods is restricted, and the resolution is too low to detect the details and abrupt changes. It is shown that wavelet is a more appropriate solution to improve the performance of TF techniques. Besides, it provides a robust framework of signal decomposition.

Developed for industrial application, a program for batch processing of WRE signals is developed in this thesis work. the Morlet wavelet is used to extract the features of WRE signals in Pre-stressed Concrete Cylinder Pipes (PCCP). The time-scale features of both WRE signals and non-WRE signals are summarized. Both of them are defined based on the previous experience obtained in industry. Also the prediction and adjustment from technicians are added into the feature summarization. With the characteristics of these features, in the form of thresholds, vast data can be auto classified into prospective categories in the developed program. In addition, the parameters and thresholds of the program are tuneable and easy to access.

After tested through industrial projects, the program based on wavelet theory is proved to be powerful to classify large quantity of data efficiently with acceptable accuracy. With the help of auto classifiers, the cost of many manual labor works and energy can be greatly reduced. In addition, the accuracy for detection of WRE signal is enhanced because analysts can concentrate on analyzing possible WRE signals avoiding fatigable works of analyzing plenty of unrelated noise signals.

In summary, wavelet analysis is an efficient technique for AE signal processing, and provides better signal detection due to its inherent ability to detect abrupt changes compared with STFT. Especially from the experimental results we can see that wavelet transform is a robust time-scale analysis for extracting detailed features.

5.2 Future Works

In the recent future, the second project discussed in this thesis needs to be completed. The result will be compared and further verified with which the auto classifiers can be improved. Then the program itself needs to be polished. Hopefully the program should be more intelligent and endue with learning ability. This means the user can build up their own libraries of features for each category, and they can reload and combine these features together to form new features for each individual project.

Another possible approach of this thesis work in future is the embedded system for

hardware implementation. The connection of the proposed algorithm with wireless communication and control is another important part in our collaboration with the pipe company. Therefore, the optimization of the proposed algorithm for hardware implementation is required in the future.

Appendix A

Abbreviation List

AET	Acoustic Emission Testing
AE	Acoustic Emission
STFT	Short-Time Fourier transform
WT	Wavelet Transform
NDT	Non-Destructive Testing
MARSE	Measured Area under the Rectified Signal Envelope
SNR	Signal to Noise Ratio
TF	Time-Frequency
TFR	Time-Frequency Representation
WD	Wigner Distribution
MP	Matching Pursuit
DWT	Discrete Wavelet Transform
CWT	Continuous Wavelet Transform
FFT	Fast Fourier Transform
IFFT	Inverse Fast Fourier Transform
PCCP	Pre-stressed Concrete Cylinder Pipe
WRE	Wire-Related Events
PDR	Power Density Ratio
LSR	Large Scale Ratio
MSR	Mid Scale Ratio
SSR	Small Scale Ratio
MA	Miss Alarm
FA	False Alarm
HYD	Hydrophone
ACC	Accelerometer

Appendix B

Introduction to the developed program

Fig. B.1 is the main user interface of the program. The interface is composed vertically of three main parts: the general settings part (in the red solid frame), the filter custom part (in the green solid frame), and the results exhibition part (in the blue solid frame). Horizontally this interface is segmented into two stages: the pre-processing stage, which is referred as PDR filtering in the program (in the dashed yellow frame); and main processing stage, which is referred as wavelet filtering in the program (in the dashed purple frame).

General Settings:

As shown in Fig. B.2, the left segment defines the overall general settings and PDR ratio information; the right segment deals with the wavelet thresholds.

- Left segment:

In the folder Info. panel: the button in the middle imports the folder that is to be processed. Or the path can be manually set in the 'Import Folder'. If the user does not want to process the whole folder, then the 'Start File' and 'End File' can be used to select those wanted files.

In the PDR settings panel: the 'Start' and 'End' refers to the samples to be calculated as the main duration, and 'Total' is the total sample number. The PDR can be manually set up, or can be generated from the 'Ratio generation' button with the 'Range' number. 'PDR

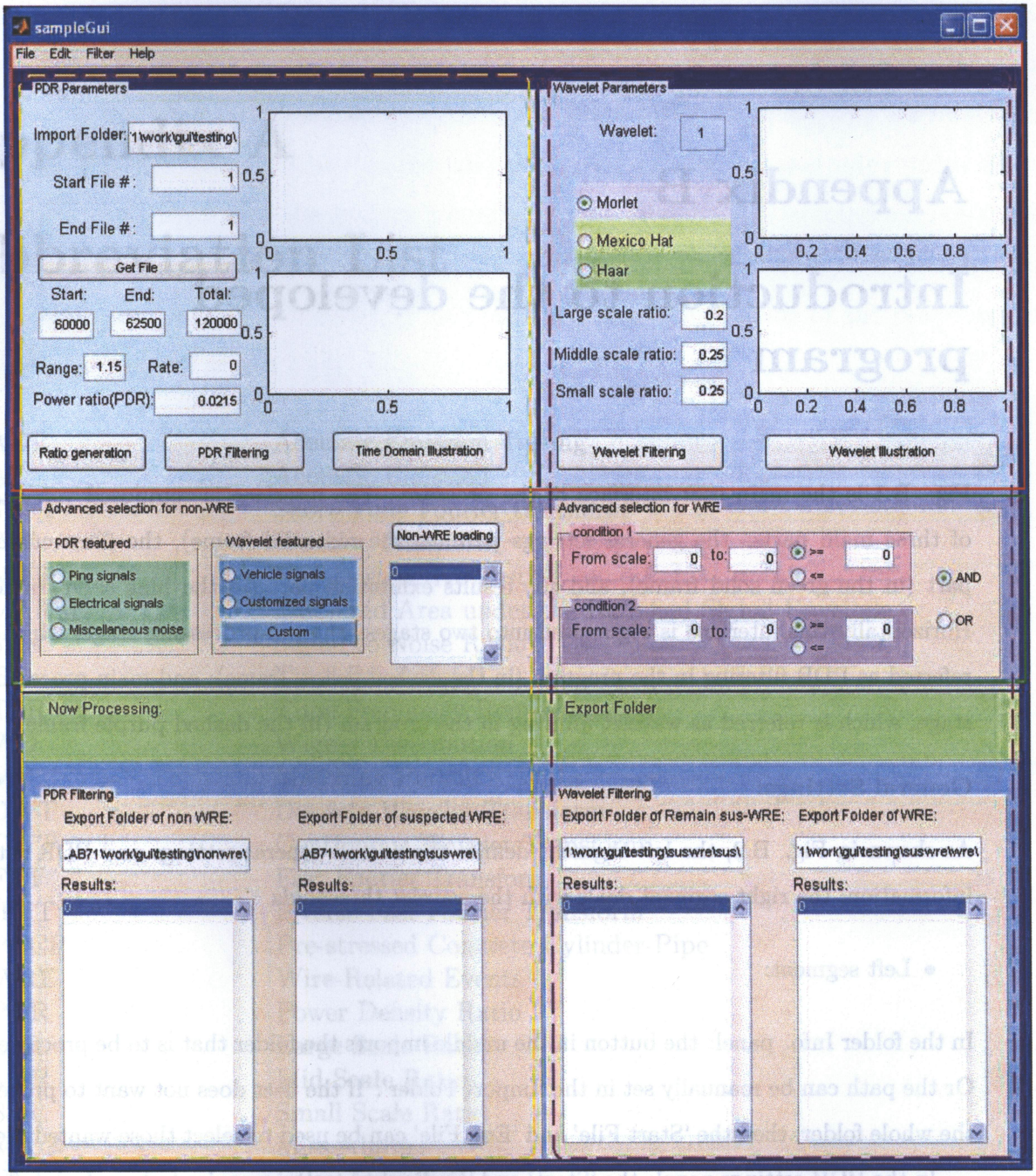

Figure B.1: A snapshot of the user interface.

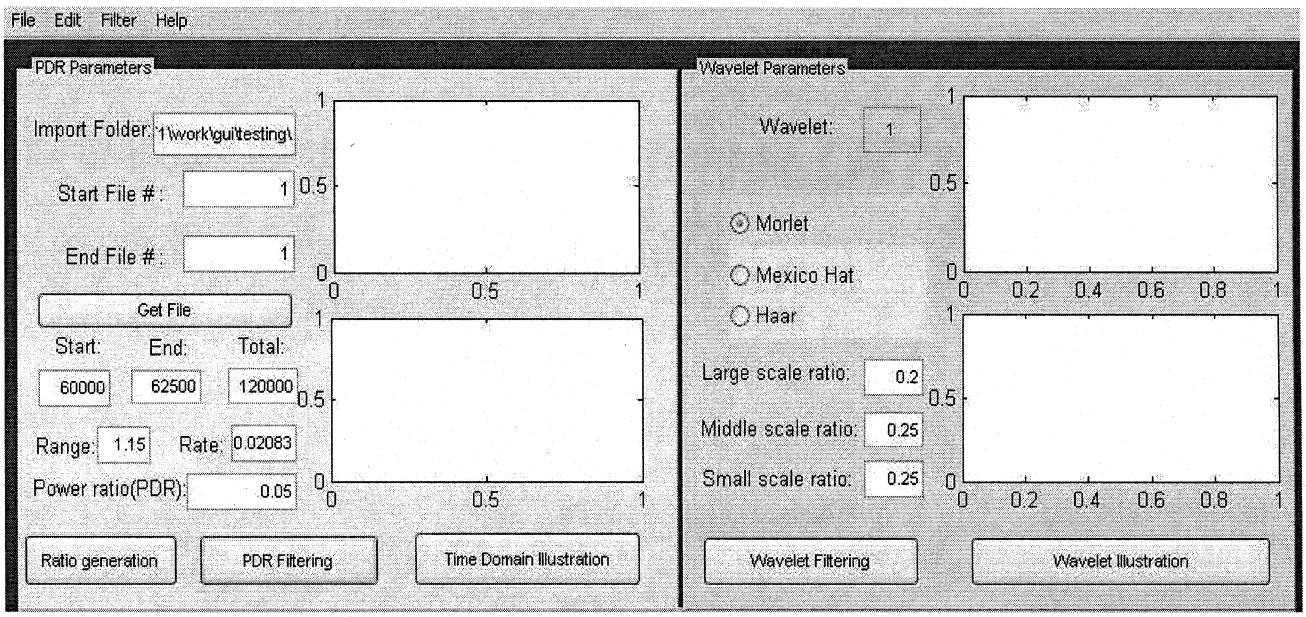

Figure B.2: The general settings part of the interface.

filtering' button does the pre-processing based on given information, and will then classify the files in the import folder into two groups: non-WRE and sus-WRE, where susWRE group refers to the files that need further process.

To show the detail of a particular signal, the time domain plot can be displayed in the two axis figures using the 'Time Domain Illustration' button. The top one is the whole time domain information, and the bottom one is the main duration part.

- Right segment:

In this segment, three wavelet functions are provided: Morlet, Mexican hat and haar wavelets. Also the default values of LSR, MSR and SSR can be changed according to different demands. The 'Wavelet filtering' button runs the main processing operation, which will further determine if the files in the sus-WRE group are real WRE or not . The 'Wavelet Illustration' gives the wavelet domain display of the selected signal.

Filter Custom:

This section allows users to omit typical non-WRE signals and to define the advanced criteria of WRE signals as shown in Fig. B.3.

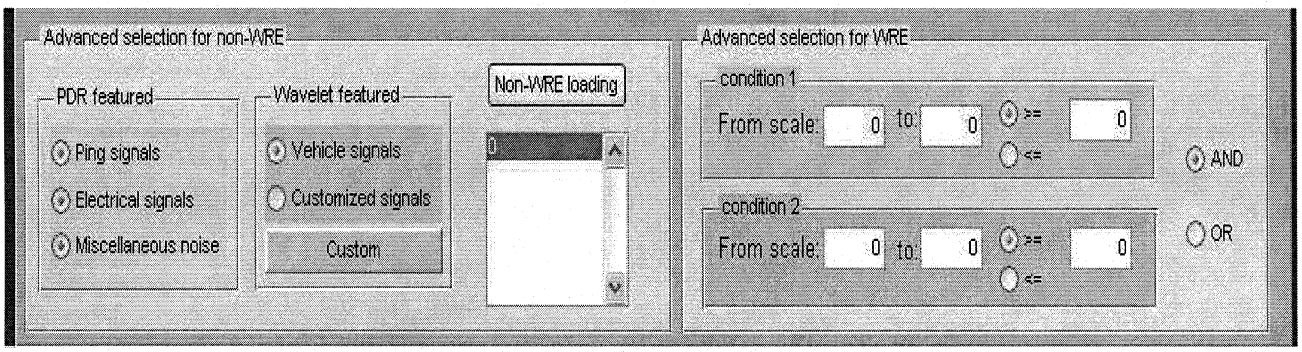

Figure B.3: The filter custom part of the interface.

- Left segment:

In the PDR featured panel: these three signals are the typical non-WRE signals that can be filtered out in the pre-processing stage as mentioned in 3.3.2.

In the wavelet featured panel: the 'vehicle signals' refer to the vehicle related sounds as described. The 'customized signals' includes the loaded signals in the listbox beside. The 'custom' button allows users to define ideal non-WRE signals which can be saved as an '.m' file. Then the 'non-WRE loading' button let users to load these defined signals and will display them in the listbox mentioned above.

These check boxes can be multi-selected or not selected at all, depending on particular requirements.

- Right segment:

Except for the three wavelet ratios shown in Fig. B.2, this segment provides two additional condition to the wavelet filtering process. Actually in some of our tested projects, a certain sort of WRE have the characteristic of focusing on two particular frequency bands. This can be result from the various physical conditions, however, the main task for our algorithm is

to detect this kind of signals. Hence more restrictions can be settled here. According to the tests, two conditions accomplished with the three wavelet ratios are adequate for the WRE signals detection. Thus in this segment, two conditions are allowed to be added with the selection of 'AND' and 'OR'.

It is easy to tell that the first two boxes are the scale range of the condition, and the third box gives the threshold. The check boxes inside the condition panels provide the selection of 'greater than' or 'less than' the threshold. While the other two check boxes outside the condition panels gives the selection of 'AND' and 'OR', which means 'both conditions must be satisfied' or 'one feature satisfied is enough'.

Results Exhibition:

This part displays the classification result and some other needed information.

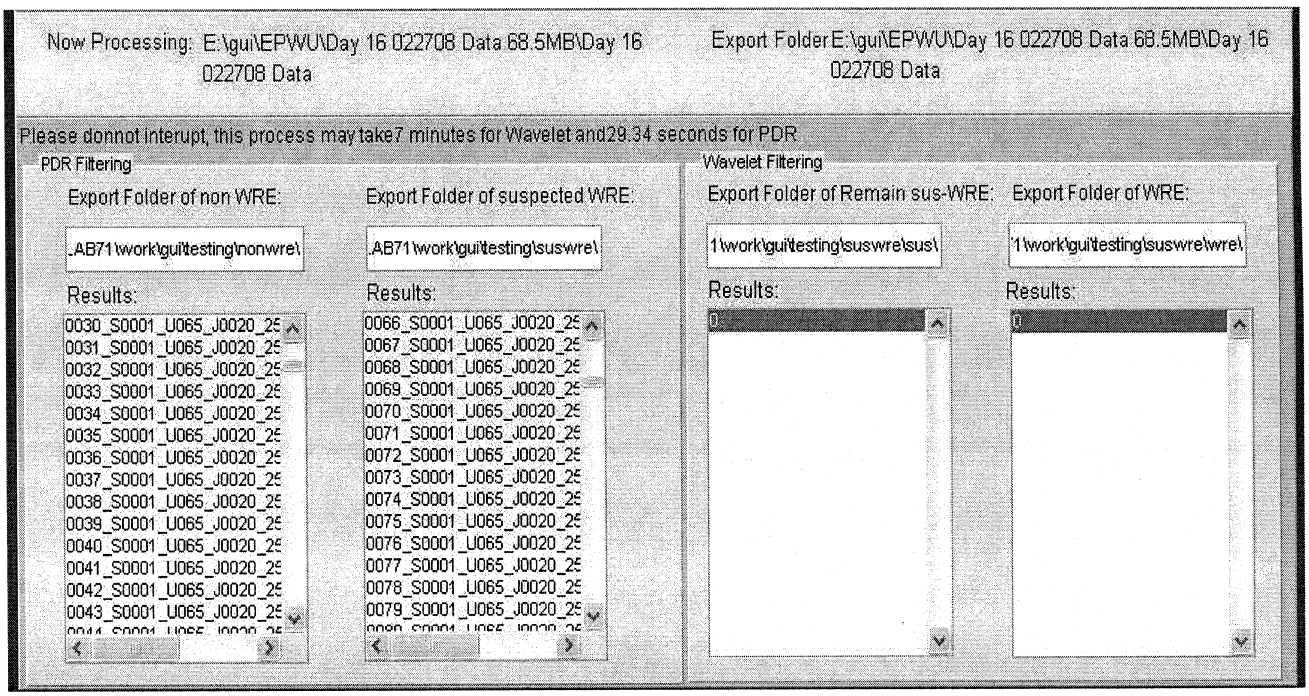

Figure B.4: The results exhibition part of the interface.

The first light green row shows the file that is in processing and the folder to hold the classified data. In addition, if the processing work is finished, and the user would like to have

a look of the time domain and wavelet domain plots, they can used the 'Illustration' buttons as shown in Fig.B.2 to display the illustrations of the file shown in this 'Now Processing'.

The following row calculates the approximate processing time of both PDR and wavelet filtering.

The last four columns are the final results of the classification. The first two columns list the results for PDR filtering which split all the data in the import folder into non-WRE and sus-WRE groups. The last two columns are the results for wavelet filtering where real WRE signals will be extracted to the 'WRE' folder and the rest signals will be left to the 'Remain sus-WRE' folder.

The default values for these four folder path are sub-folders of the 'Export Folder', which is shown at the first row of this part. These path also can be changed manually as users wishes.

Bibliography

[1] J. F. Stulen and F. B. Kiefner, "Evaluation of acoustic emission monitoring of buried pipelines," *IEEE Trans. Ultronics Symposium*, vol. 90, pp. 898–903, 1982.

[2] J. R. Smith, G. V. Rao, and R. Gopal, "Acoustic monitoring for leak detection in pressurized water reactors," *ASTM. Special Technical Publications*, pp. 177–204, Jan. 1979.

[3] K. Yoshida, H. Kawano, Y. Akematsu, and H. Nishino, "Frequency characteristics of acoustic emission waveforms during gas leak," *The European Working Group on Acoustic Emission*, 2004.

[4] V. V. Muravev, M. V. Muravev, and S. A. Bekher, "A novel technique of AE signal processing for upgrading the accuracy of flaw localization," *Acoustic methods, Russian journal of nondestructive testing*, vol. 38, no. 8, pp. 600–610, Aug. 2002.

[5] B. Frielander and B. Porat, "Detection of transient signals by Gabor representation," *IEEE Trans. Acoustics, Speech and Signal Processing*, vol. 37, no. 2, pp. 169–180, 1989.

[6] D. Gabor, "Theory of communication," *IEEE Trans, Communications*, vol. 93, pp. 424–441, 1996.

[7] C. Macia-Sanahuja and H. Lamela-Rivera, "Wavelet analysis of partial discharges acoustic waves obtained using an optical fibre interferometric sensor for transformer applications," *Industrial Electronics, ISIE-03*, vol. 2, pp. 1071–1076, June 2003.

[8] R. Sabbah, J. Verdenet, M. baud, O. Blagosklonov, L. Comas, and J.C.Cardot, "using wavelets for smoothing and denoising gated blooded pool images," *Computers in Cardiology,*, pp. 189–192, Sept 2002.

[9] B. L. Li and H. Wu, "Change detection in nonlinear biosignal processing by wavelets," *Biomedical Engineering Conference*, pp. 307–310, March 1996.

[10] M. Akay, "Wavelet applications in medicine," *Spectrum, IEEE*, vol. 34, pp. 50–56, May 1997.

[11] R. D. Priebe and G. R. Wilson, "Wavelet applications to structural analysis," *Acoustics, Speech and Signal Processing, ICASSP-94*, vol. 3, pp. 205–208, April 1994.

[12] R. Diederichs, "Nondestructive testing," *http://www.ndt.net/ndtaz/ndtaz.php*, July 2007.

[13] C. U. Grosse, "Editorial: Special issue on acoustic emission," *NDT.net*, vol. 7, no. 9, Sept 2002.

[14] "What is acoustic emission," *http://www.ndt.net/article/az/ae_idx.htm.*

[15] G. Lackner, G. Schauritsch, and P. Tsheliesnig, "Acoustic emission: a mordern and common NDT method to estimate industrial facilities," *ECNDT 2006*, 2006.

[16] H. Vallen, "Ae testing fundamentals,equipment, applications," *NDT.net*, vol. 7, no. 9, Sept 2002.

[17] M. Peacock, "Acoustic emission for detection of process related damage in pressure vessels and piping," *SPIE*, vol. 2947, 1996.

[18] S. P. Ebenezer, A. P. Suppappola, and S. B. Suppappola, "Classification of acoustic emissions using modified matching pursuit," *Journal on Applied Signal Processing, EURASIP*, pp. 347–357, March 2004.

[19] L. Cohen, *Time-Frequency Analysis*, Prentice Hall, NJ, USA, 1995.

[20] P. Flandrin, *Time-Frequency/Time-Scale Analysis*, Academic Press, Calif ,USA, 1999.

[21] F. Hlawatsch and G. F. Boudreaux-Bartels, "Linear and quadratic time-frequency signal representations," *IEEE Signal Processing Magazine*, vol. 9, no. 2, pp. 21–67, 1992.

[22] S. Mallat and Z. Zhang, "Matching pursuit with time-frequency dictionaries," *IEEE Transactions on Signal Processing*, vol. 41, no. 12, pp. 3397–3415, Dec 1993.

[23] S. Qian, D. Chen, and K.Chen, "Signal approximation via data-adaptive normalized gaussian function and its applications for speech processing," *ICASSP*, pp. 141–144, March 1992.

[24] S. Mallat and Z. Zhang, "The matching pursuit software package," *ftp://cs.nyu.edu/pub/wave/software/mpp.tar.Z.*

[25] A. P. Suppappola and S. B. Suppappola, "Adaptive time-frequency representations for multiple structures," *10th IEEE Workshop on Statistical Signal and Array Processing*, pp. 579–583, Aug 2000.

[26] C. Valens, "A really friendly guide to wavelets," *http://www.cs.unm.edu/~williams/cs530/arfgtw.pdf*, 1999.

[27] R. Wu, Z. Liao, L. Zhao, and X. Kong, "Wavelets application in acoustic emission signal detection of wire related events in pipeline," *Canadian Acoustics*, p. to appear, June 2008.

[28] R. Wu, Z. Liao, L. Zhao, and X. Kong, "Wavelets application on acoustic emission signal detection in pipeline," *CCECE'08*, p. to appear, May 2008.

[29] "Evaluation and repair of the ullrich medium service transmission main," *http://www.ctlgroup.com*, 2007.

[30] T. Boczar and D. Zmarzly, "Application of wavelet analysis to acoustic emission pulses generated by partial discharges," *IEEE Trans. Dielectics and Electrical Insulation*, vol. 11, no. 3, 2004.

[31] S. Mallat, *A wavlet tour of signal processing*, Academic Press, 1998.

[32] G. Kaiser, *A Friendly Guide to Wavelets*, Birkhauser, 1994.

[33] C. Torrence and G. P. Compo, "A practical guide to wavelet analysis," *Bulletin of the American Meteorological Society*, vol. 79, no. 1, Jan. 1998.

[34] M. Frage, "Wavelet transforms and their applications to turbulence," *Annu. Rev. Fluid Mech.*, vol. 24, pp. 395–457, 1992.

[35] A. Boggess and F. J. Narcowich, *A first course in wavelets with Fourier analysis*, Prentice Hall, 2004.

[36] H. G. Stark, *Wavelets and signal processing*, Springer, 2005.